

Articles

Synthesis and Structure of New Neutral Bimetallic Platinum Hydride Complexes

Irene Ara,[†] Larry R. Falvello,[†] Juan Forniés,^{*,†} Elena Lalinde,^{*,‡}
Antonio Martín,[†] Francisco Martínez,[†] and M. Teresa Moreno[‡]

Departamento de Química Inorgánica, Instituto de Ciencia de Materiales de Aragón,
Universidad de Zaragoza-Consejo Superior de Investigaciones Científicas, 50009 Zaragoza,
Spain, and Departamento de Química, Universidad de La Rioja, 26001 Logroño, Spain

Received July 9, 1997[©]

The reactions of mononuclear hydride complexes *trans*-[PtHXL₂] with the solvated species *cis*-[Pt(C₆F₅)₂(thf)₂] constitute a simple methodology to high-yield synthesis of dinuclear compounds with a mixed bridging system H/X. Thus, *trans*-[Pt(C≡CPh)H(PPh₃)₂] reacts readily with *cis*-[Pt(C₆F₅)₂(thf)₂] to give *trans*-[(C₆F₅)(PPh₃)Pt(*μ*-H)(*μ*-C≡CPh)Pt(C₆F₅)(PPh₃)] (**1b**), containing (X-ray) a *μ*-η¹:η²-C≡CPh alkynyl ligand. *trans*-[Pt(C₆F₅)H(PPh₃)₂] reacts with *cis*-[Pt(C₆F₅)₂(thf)₂] under mild conditions to afford initially the 1:1 adduct *trans*,*cis*-[(C₆F₅)(PPh₃)Pt(*μ*-H)(*μ*(*P*-η²-PPh₃)Pt(C₆F₅)₂)] (**2a**), which finally rearranges quantitatively to form *cis*-[(C₆F₅)(PPh₃)Pt(*μ*-H)(*μ*-C₆F₅)Pt(C₆F₅)(PPh₃)] (**2c**). The crystal structures of **2a**, a compound displaying an unusual PPh₃ bridging ligand *via* the P donor atom and an η²-phenyl interaction, and **2c** with a mixed pentafluorophenyl/hydride bridged system are reported. Similar hydride/chloride bridged diplatinum complexes [(C₆F₅)LPt(*μ*-H)(*μ*-Cl)Pt(C₆F₅)L] (**3**, L = PPh₃; **4**, L = PEt₃), are also quantitatively formed by treatment of *trans*-[PtClHL₂] with *cis*-[Pt(C₆F₅)₂(thf)₂] in CHCl₃. Both complexes are obtained as *trans* isomers (**3b** and **4b**), but their NMR data in CD₃COCD₃ indicate that they are present as a mixture of *trans* (**3b**, **4b**) and *cis* (**3c**, **4c**) isomers. Slow crystallization of **3b** (CH₂Cl₂/hexane) in the presence of light gave crystals of the *cis* isomer **3c** (X-ray), which is also quantitatively formed by photolysis of **3b**. The presence of hydride bridging ligands in all complexes **1–4** is unambiguously confirmed by ¹H NMR spectroscopy.

Introduction

Bimetallic hydride-bridged complexes are an interesting family of compounds because of their structural features and reactivity, particularly as related to their catalytic activity.¹ Since the report of the first neutral doubly hydride bridged diplatinum complexes [Pt(*μ*-H)-RL₂]₂ (R = H, SiR'₃, GeR'₃, L = phosphine),² which were shown to be very efficient catalysts for the hydrosilylation and hydrogermylation of alkenes and alkynes,³ several types of homodinuclear hydride-bridged platinum compounds have been reported. In the most

common type the platinum atoms are linked only by hydride ligands, and examples of both singly (*μ*-H)⁴ and doubly (*μ*-H)₂^{4dffi,5} hydride bridged derivatives are known. Hydride-bridged complexes containing other bridging ligands, the latter contributing to the reinforcement of the stability of the dinuclear unit, are also known; the most representative are the cationic bis(diphenylphosphino)methane-bridged A-frame species of type [Pt₂X₂(*μ*-H)(*μ*-dppm)₂]⁺ (X = halide, hydride, alkyl, aryl, alkynyl).⁶ In contrast, examples of diplatinum complexes containing a mixed-bridge system of the type

[†] Universidad de Zaragoza-Consejo Superior de Investigaciones Científicas.

[‡] Universidad de La Rioja.

[©] Abstract published in *Advance ACS Abstracts*, November 1, 1997.

(1) (a) Venanzi, L. M. *Coord. Chem. Rev.* **1982**, *43*, 251. (b) Hlatki, G. G.; Crabtree, R. H. *Coord. Chem. Rev.* **1985**, *65*, 1; *Comments Inorg. Chem.* **1985**, *4*, 229. (c) Chaloupka, S.; Venanzi, L. M. *Inorg. Synth.* **1990**, *27*, 30. (d) Boag, N. M.; Browning, J.; Crocker, C.; Goggin, P. L.; Goodfellow, R. J.; Murray, M.; Spencer, J. L. *J. Chem. Res., Synop.* **1978**, 228; *J. Chem. Res., Miniprint* **1978**, 2962. (e) Albinati, A.; Chaloupka, S.; Demartin, F.; Koetzle, T. F.; Ruegger, H.; Venanzi, L. M.; Wolfer, M. K. *J. Am. Chem. Soc.* **1993**, *115*, 168 and references quoted therein.

(2) (a) Green, M.; Howard, J. A. K.; Proud, J.; Spencer, J. L.; Stone, F. G. A.; Tsipis, A. C. *J. Chem. Soc., Chem. Commun.* **1976**, 671. (b) Ciriano, M.; Green, M.; Howard, J. A. K.; Proud, J.; Spencer, J. L.; Stone, F. G. A.; Tsipis, C. A. *J. Chem. Soc., Dalton Trans.* **1978**, 801.

(3) Green, M.; Spencer, J. L.; Stone, F. G. A.; Tsipis, C. A. *J. Chem. Soc., Dalton Trans.* **1977**, 1519–1525, 1525–1529. (b) Tsipis, C. A. *J. Organomet. Chem.* **1980**, *188*, 53–61; **1980**, *187*, 427–446.

(4) (a) Bracher, G.; Grove, D. M.; Venanzi, L. M.; Bachechi, F.; Mura, P.; Zambonelli, L. *Angew. Chem., Int. Ed. Engl.* **1978**, *17*, 778. (b) Minghetti, G.; Banditelli, G.; Bandini, A. L. *J. Organomet. Chem.* **1977**, *139*, C80. (c) Tulip, T. H.; Yamagata, T.; Yoshida, T.; Wilson, R. D.; Ibers, J. A.; Otsuka, S. *Inorg. Chem.* **1979**, *18*, 2239. (d) Grove, D. M.; van Koten, G.; Ubbels, H. J. C. *J. Am. Chem. Soc.* **1982**, *104*, 4285. (e) Carmona, D.; Thouvenot, R.; Venanzi, L. M.; Bachechi, F.; Zambonelli, L. *J. Organomet. Chem.* **1983**, *250*, 589. (f) Paonessa, R. S.; Trogler, W. C. *Inorg. Chem.* **1983**, *22*, 1038. (g) Carmona, D.; Chaloupka, S.; Jans, J.; Thouvenot, R.; Venanzi, L. M. *J. Organomet. Chem.* **1984**, *275*, 303. (h) Paonessa, R. S.; Prignano, A. L.; Trogler, W. C. *Organometallics* **1985**, *4*, 647. (i) Bandini, A. L.; Banditelli, G.; Cinellu, M. A.; Sanna, G.; Minghetti, G.; Demartin, F.; Manassero, M. *Inorg. Chem.* **1989**, *28*, 404. (j) Bergamini, P.; Sostero, S.; Traverso, O.; Venanzi, L. M. *Inorg. Chem.* **1990**, *29*, 4376. (k) Bachechi, F. *Acta Crystallogr.* **1993**, *C49*, 460. (l) Bachechi, F.; Mura, P.; Zambonelli, L. *Acta Crystallogr.* **1993**, *C49*, 2072. (m) Schwartz, D. J.; Andersen, R. A. *J. Am. Chem. Soc.* **1995**, *117*, 4014. (n) Hill, G. S.; Puddephatt, R. J. *J. Am. Chem. Soc.* **1996**, *118*, 8745. (o) Albinati, A.; Chaloupka, S.; Eckert, J.; Venanzi, L. M.; Wolfer, M. K. *Inorg. Chim. Acta* **1997**, *259*, 305.

Pt(μ -H)(μ -X)Pt are relatively scarce.⁷⁻⁹ As far as we are aware, only three dimeric derivatives with a mixed hydride/phosphide bridging system have been reported—[Pt(Ph₂POHOPPh₂)Pt]₂(μ -H)(μ -PPh₂),^{8c} [L₂Pt(μ -H)(μ -PR')Pt(LR)]⁺ (L = PPh₃, R' = R = Ph;^{8a,b} L = PHBu^t₂, R' = Bu^t, R = H^{8d})—in addition to several cationic derivatives [Pt₂(μ -H)(μ -X)(L-L)₂]⁺ synthesized by Minghetti *et al.*,^{4i,7} which are formally diplatinum(I) species. A serendipitous preparation of [Pt₂(μ -H)(μ -S)(dppe)₂]PF₆ has also been reported.^{9a,b} Our interest in platinum hydride complexes arises from the reported unexpected formation of a μ -phenylethenylidene-bridged diplatinum complex by direct reaction between the alkynyl-hydride mononuclear complexes *trans*-[Pt(C \equiv CPh)H(PPh₃)₂] and *cis*-[Pt(C₆F₅)₂(thf)(CO)].¹⁰ In this paper we report the synthesis and structural characterization of novel neutral diplatinum complexes [Pt₂(μ -X)(μ -H)(C₆F₅)₂L₂] (L = PPh₃, X = C \equiv CPh (**1b**), C₆F₅ (**2c**), Cl (**3b,c**); L = PEt₃, X = Cl (**4b,c**)) displaying three new mixed hydride bridging systems. These complexes are obtained in quantitative yield from simple reactions of *cis*-[Pt(C₆F₅)₂(thf)₂] with mononuclear hydride species *trans*-[PtXHL₂]. In addition, we also report the isolation of an unexpected intermediate isomeric precursor in the formation of **2c**, *trans,cis*-[(C₆F₅)(PPh₃)Pt(μ -H)(μ -P)- η^2 -PPh₃)Pt(C₆F₅)₂] (**2a**), which displays (X-ray) an unusual μ (P)- η^2 -tri-phenylphosphine bridging ligand.

(5) (a) Bracher, G.; Grove, D. M.; Pregosin, P. S.; Venanzi, L. M. *Angew. Chem., Int. Ed. Engl.* **1979**, *18*, 155; *Angew. Chem.* **1979**, *91*, 169. (b) Paonessa, R. S.; Trogler, W. C. *J. Am. Chem. Soc.* **1982**, *104*, 3529. (c) Bachechi, F.; Bracher, G.; Grove, D. M.; Kellenberger, B.; Pregosin, P. S.; Venanzi, L. M.; Zambonelli, L. *Inorg. Chem.* **1983**, *22*, 1031. (d) Knobler, C. B.; Kaesz, H. D.; Minghetti, G.; Bandini, A. L.; Banditelli, G.; Bonati, F. *Inorg. Chem.* **1983**, *22*, 2324. (e) Packett, D. L.; Syed, A.; Trogler, W. C. *Organometallics* **1988**, *7*, 159. (f) Carmichael, D.; Hitchcock, P. B.; Nixon, J. F.; Pidcock, A. *J. Chem. Soc., Chem. Commun.* **1988**, 1554. (g) Aime, S.; Gobetto, R.; Bandini, A. L.; Banditelli, G.; Minghetti, G. *Inorg. Chem.* **1991**, *30*, 316. (h) Bennett, B. L.; Roddick, D. M. *Inorg. Chem.* **1996**, *35*, 4703 and references given therein. (i) Mole, L.; Spencer, J. L.; Litster, S. A.; Redhouse, A. D.; Carr, N.; Orpen, A. G. *J. Chem. Soc., Dalton Trans.* **1996**, 2315.

(6) (a) Brown, M. P.; Puddephatt, R. J.; Rashidi, M.; Seddon, K. R. *J. Chem. Soc., Dalton Trans.* **1978**, 516; *Inorg. Chim. Acta* **1977**, *23*, L27. (b) Brown, M. P.; Cooper, S. J.; Frew, A. A.; Manojlovic-Muir, L.; Muir, K. W.; Puddephatt, R. J.; Thomson, M. A. *J. Chem. Soc., Dalton Trans.* **1982**, 299; *J. Organomet. Chem.* **1980**, *198*, C33. (c) Azam, K. A.; Puddephatt, R. J. *Organometallics* **1983**, *2*, 1396. (d) Azam, K. A.; Brown, M. P.; Cooper, S. J.; Puddephatt, R. J. *Organometallics* **1982**, *1*, 1183. (e) Grossel, M. C.; Batson, R. J.; Moulding, R. P.; Seddon, K. K. *J. Organomet. Chem.* **1986**, *304*, 391. (f) Langrick, C. R.; Pringle, P. G.; Shaw, B. L. *J. Chem. Soc., Dalton Trans.* **1985**, 1015. (g) Anderson, G. K. *Adv. Organomet. Chem.* **1993**, *35*, 1. (h) Xu, C.; Anderson, G. K. *Organometallics* **1994**, *13*, 3981. (i) Xu, C.; Anderson, G. K. *Organometallics* **1996**, *15*, 1760.

(7) (a) Minghetti, G.; Bandini, A. L.; Banditelli, G.; Bonati, F. *J. Organomet. Chem.* **1979**, *179*, C13. (b) Minghetti, G.; Bandini, A. L.; Banditelli, G.; Bonati, F.; Szostak, R.; Strouse, C. E.; Knobler, C. B.; Kaesz, H. D. *Inorg. Chem.* **1983**, *22*, 2332. (c) Minghetti, G.; Albinati, A.; Banditelli, G. *Angew. Chem., Int. Ed. Engl.* **1985**, *24*, 120.

(8) (a) Jans, J.; Naegeli, R.; Venanzi, L. M.; Albinati, A. *J. Organomet. Chem.* **1983**, *247*, C37. (b) Siedle, A. R.; Newmark, R. A.; Gleason, W. B. *J. Am. Chem. Soc.* **1986**, *108*, 767. (c) van Leeuwen, P. W. N. M.; Roobeek, C. F.; Frijns, J. H. G.; Orpen, A. G. *Organometallics* **1990**, *9*, 1211. (d) Leoni, P.; Manetti, S.; Pascuali, M. *Inorg. Chem.* **1995**, *34*, 749.

(9) (a) Capdevila, M.; González-Duarte, P.; Mira, I.; Sola, J.; Glegg, W. *Polyhedron* **1992**, *12*, 3091. (b) Glegg, W.; Capdevila, M.; González-Duarte, P.; Sola, J. *Acta Crystallogr.* **1996**, *B52*, 270. (c) The species [(L-L)₂Pt₂(μ -Cl)(μ -H)]²⁺ (L-L = (C₆H₁₁)₂PCH₂CH₂P(C₆H₁₁)₂) has also been noted to be formed (¹H, ³¹P) by crystallization of [Pt(C₇H₁₁)(L-L)]⁺ in chlorinated solvents: Carr, N.; Dunne, B. J.; Mole, L.; Orpen, A. G.; Spencer, J. L. *J. Chem. Soc., Dalton Trans.* **1991**, 863.

(10) Ara, I.; Berenguer, J. R.; Forniés, J.; Lalinde, E.; Tomás, M. *Organometallics* **1996**, *15*, 1014.

Results and Discussion

It is now well-established that *cis*-[Pt(C₆F₅)₂(thf)₂]¹¹ is an excellent precursor to a variety of mono-,^{12a-g} di-,^{12h-m} and polynuclear^{12n-q} complexes containing the “*cis*-Pt(C₆F₅)₂” fragment, since the two thf groups are easily replaced by other ligands.¹² In the preparation of di- and polynuclear derivatives much of the effort with *cis*-[Pt(C₆F₅)₂(thf)₂] has focused on the study of its reactivity toward metallo species with potentially bridging groups in *cis* positions and, probably because of that, the reactions always proceed with stereoretention. The reactivity of *cis*-[Pt(C₆F₅)₂(thf)₂] toward metallo species with the potentially bridging ligands in a relative *trans* disposition has been scarcely explored,^{13ab} but we recently noted the different behavior of *cis*-[Pt(C₆F₅)₂(thf)₂] toward neutral bis(alkynyl) mononuclear platinum complexes.^{13a} Thus (Scheme 1), while the reactions with *cis*-[Pt(C \equiv CR)₂(PPh₃)₂] take place, as expected, with retention of the *cis* geometry around both platinum centers, yielding asymmetric complexes *cis,cis*-[Pt₂(μ -C \equiv CR)₂](C₆F₅)₂¹²ⁱ (Scheme 1i), the analogous reactions with the *trans* derivatives result in a redistribution of ligands and the ultimate formation of the symmetric *trans*-[Pt(C \equiv CR)(C₆F₅)(PPh₃)₂]₂^{13a} (Scheme 1ii). Therefore, we considered it of interest to explore this synthetic approach to dinuclear derivatives containing a mixed bridging system, and in view of the rather small number of hydride-bridged diplatinum complexes of the type Pt(μ -H)(μ -X)Pt we sought first to utilize this strategy with mononuclear hydride complexes of the type *trans*-[PtXHL₂] (X = C \equiv CPh, Cl, C₆F₅). In all cases, the reactions with *cis*-[Pt(C₆F₅)₂(thf)₂] lead to the formation of dimetallic hydride-bridged complexes, as is observed by NMR spectroscopy.

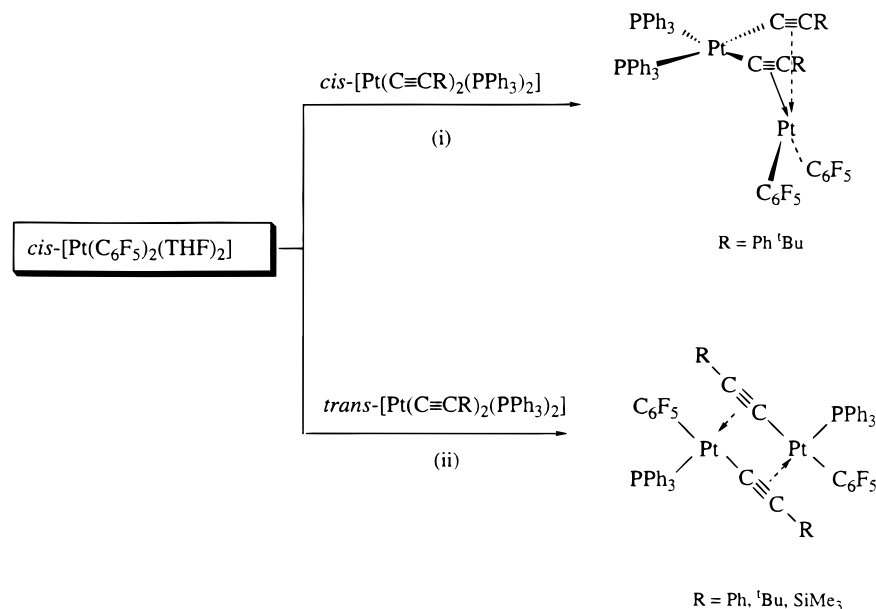
Reaction of *cis*-[Pt(C₆F₅)₂(thf)₂] with *trans*-[Pt(C \equiv CPh)H(PPh₃)₂]. Treatment of *trans*-[Pt(C \equiv CPh)H(PPh₃)₂] with *cis*-[Pt(C₆F₅)₂(thf)₂] in CHCl₃ at room temperature affords *trans*-[(C₆F₅)(PPh₃)Pt(μ -H)-(μ (σ , π)- η^2 -C \equiv CPh)Pt(C₆F₅)(PPh₃)] (**1b**), isolated in 75% yield, which is the first example of a diplatinum complex with a mixed μ -H, μ -C \equiv CPh bridging system (Scheme

(11) Usón, R.; Forniés, J.; Tomás, M.; Menjón, B. *Organometallics* **1985**, *4*, 1912.

(12) (a) Casas, J. M.; Falvello, L. R.; Forniés, J.; Martín, A. *Inorg. Chem.* **1996**, *35*, 56 and references given therein. (b) Casas, J. M.; Forniés, J.; Martín, A.; Menjón, B.; Tomás, M. *J. Chem. Soc., Dalton Trans.* **1995**, 2949. (c) Casas, J. M.; Forniés, J.; Martín, A.; Menjón, B. *Organometallics* **1993**, *12*, 4376. (d) Forniés, J.; Menjón, B.; Gómez, N.; Tomás, M. *Organometallics* **1992**, *11*, 1187. (e) Usón, R.; Forniés, J.; Tomás, M.; Menjón, B.; Welch, A. J. *J. Organomet. Chem.* **1986**, *304*, C24. (f) Usón, R.; Forniés, J.; Tomás, M.; Menjón, B.; Fortuño, C.; Welch, A. J.; Smith, D. E. *J. Chem. Soc., Dalton Trans.* **1993**, 275. (g) Usón, R.; Forniés, J.; Tomás, M.; Menjón, B. *Organometallics* **1986**, *5*, 1581. (h) Usón, R.; Forniés, J.; Tomás, M.; Casas, J. M.; Navarro, R. *J. Chem. Soc., Dalton Trans.* **1989**, 169. (i) Forniés, J.; Gómez-Saso, M. A.; Lalinde, E.; Martínez, F.; Moreno, M. T. *Organometallics* **1992**, *11*, 2873. (j) Berenguer, J. R.; Falvello, L. R.; Forniés, J.; Lalinde, E.; Tomás, M. *Organometallics* **1993**, *12*, 6. (k) Forniés, J.; Lalinde, E.; Martín, A.; Moreno, M. T.; Welch, A. J. *J. Chem. Soc., Dalton Trans.* **1995**, 1333. (l) Delgado, E.; Forniés, J.; Hernández, E.; Lalinde, E.; Mansilla, N.; Moreno, M. T. *J. Organomet. Chem.* **1995**, *494*, 261. (m) Amador, U.; Delgado, E.; Forniés, J.; Hernández, E.; Lalinde, E.; Moreno, M. T. *Inorg. Chem.* **1995**, *34*, 5279. (n) Forniés, J.; Martínez, F.; Navarro, R.; Urriolabeitia, E. P.; Welch, A. J. *J. Chem. Soc., Dalton Trans.* **1995**, 2805. (o) Usón, R.; Forniés, J.; Tomás, M.; Menjón, B.; Welch, A. J. *Organometallics* **1988**, *7*, 1318. (p) Usón, R.; Forniés, J.; Tomás, M.; Menjón, B.; Carnicer, J.; Welch, A. J. *J. Chem. Soc., Dalton Trans.* **1990**, 151. (q) Forniés, J.; Lalinde, E.; Martín, A.; Moreno, M. T. *J. Chem. Soc., Dalton Trans.* **1994**, 135.

(13) (a) Berenguer, J. R.; Forniés, J.; Martínez, F.; Cubero, J. C.; Lalinde, E.; Moreno, M. T.; Welch, A. J. *Polyhedron* **1993**, *12*, 1797. (b) Usón, R.; Forniés, J.; Usón, M. A.; Mas, M. L. *Inorg. Chim. Acta* **1990**, *168*, 59.

Scheme 1



2, i). Species in which the metal centers are connected only through a mixed $\mu\text{-H}$, $\mu\text{-C}\equiv\text{CR}$ bridging system are rather rare.¹⁴ When the reaction is monitored by NMR spectroscopy, it is observed that the formation of complex **1b** is immediate (1 or 2 min) and complete; no other compound is present in solution (¹H, ³¹P, and ¹⁹F NMR). Complex **1b** is indefinitely stable both in the solid state and in solution and has been characterized by microanalysis and IR and NMR spectroscopy; finally, a definitive structural assignment has been established by X-ray crystallography. In the IR spectrum of **1b** a weak absorption at 2018 cm⁻¹, which we assign to $\nu(\text{C}\equiv\text{C})$, indicates the presence of a bridging alkynyl ligand.^{12i,q,13a} We have made no attempts to locate the IR absorption of the bridging hydride, as it is well-known that such absorptions ($\sim 1600\text{ cm}^{-1}$) are usually weak and often difficult to assign.¹⁵ The ¹⁹F NMR spectrum (see Experimental Section) shows two sets of signals ($2F_o$, F_p , $2F_m$), confirming that the two C₆F₅ groups are inequivalent. The dimeric nature of the complex is apparent from the ³¹P and ¹H NMR spectra, each of which consists of the superposition of three subspectra, arising from the three different isotomeric combinations of platinum nuclei having different nuclear spins (Pt/Pt 43.8%, ¹⁹⁵Pt/Pt 22.4%, Pt/¹⁹⁵Pt 22.4% and ¹⁹⁵Pt/¹⁹⁵Pt 11.4%, the percentages arising from the 33.8% natural abundance of ¹⁹⁵Pt). The ³¹P NMR spectrum shows, as expected, two resonances, each exhibiting short and long platinum satellites ($\delta[\text{P}(1)]$ 29.21, ¹ $J_{\text{Pt}(1)\text{-P}(1)} = 3843$ and $J_{\text{Pt}(2)\text{-P}(1)} = 101$ Hz; $\delta[\text{P}(2)]$ 11.30, ¹ $J_{\text{Pt}(2)\text{-P}(2)} = 3590$ and $J_{\text{Pt}(1)\text{-P}(2)} \approx 30$ Hz with $J_{\text{P}(1)\text{-P}(2)} \approx 0$), in agreement with the presence of two inequivalent phosphorus nuclei (see Table 1 for nuclei labeling). Resonances due to P(1) and P(2) have been

unambiguously assigned by observing the ³¹P NMR spectrum while decoupling only the triphenylphosphine protons. With this treatment, the downfield signal ($\delta[\text{P}(1)]$ 29.21) clearly splits into a doublet ($J \approx 73$ Hz) by the large expected coupling to the *trans* bridging hydride. The resonance centered at δ 11.3 is not affected and is therefore assigned to the PPh₃ ligand (P(2)) which is *cis* to the hydride ligand. The ¹H NMR spectrum unequivocally demonstrates the presence of a bridging hydride ligand. It exhibits in the high-field region (see Figure 1) one hydride resonance at -7.44 ppm with different coupling constants to the two inequivalent ³¹P nuclei (² $J_{\text{H-P}(1)(\text{trans})} = 74.2$ Hz, ² $J_{\text{H-P}(2)(\text{cis})} = 14.5$ Hz). Moreover, this resonance shows two different sets of ¹⁹⁵Pt satellites, which establishes that this hydride, not observed in the X-ray crystal structure (see below), bridges the two platinum atoms. The whole resonance has roughly the appearance of a quintet (1:8:18:8:1) of multiplets (dd central (18) and outer (1) signals and overlapping of dd for the remaining (4:4)), thus proving the presence of a Pt₂($\mu\text{-H}$) group.^{4n,6a,b} The magnitudes of both ¹ $J_{\text{Pt-H}}$ values (562 and 515 Hz, respectively) are in the range previously found in other hydride-diplatinum derivatives.⁴⁻⁸ In the ¹³C NMR spectrum the acetylenic carbon signals are observed at 108.7 and 124.9 ppm for C_α and C_β, respectively, which compares well with the values given for dinuclear derivatives of other metals containing an analogous $\mu\text{-H}$, $\mu\text{-C}\equiv\text{CR}$ mixed bridging system.¹⁴ In order to determine the structure of **1b**, an X-ray diffraction study of a single crystal has been carried out. A view of the skeleton of the molecule is shown in Figure 2, and selected bond distances and angles are listed in Table 2. As can be seen, the heavy-atom skeleton confirms its dinuclear nature formed by two Pt(C₆F₅)(PPh₃) units connected by the alkynyl ligand which is σ -bonded to Pt(1) (Pt(1)–C(1) = 1.98(2) Å) and unsymmetrically η^2 -bonded to Pt(2) with the α -carbon atom closer to Pt(2) (Pt(2)–C(1) = 2.23(1) Å) than the C_β atom (Pt(2)–C(2) = 2.35(1) Å). This type of asymmetry is opposite to that found in the neutral doubly alkynyl bridged complex [Pt($\mu(\sigma)\text{-}\eta^2\text{-C}\equiv\text{CPh}$)(C₆F₅)(PPh₃)₂]₂,^{13a} and in accord with this structural feature, the Pt(1)–C(1)–Pt(2) angle (83.8(5)°) is

(14) (a) Nubel, P. O.; Brown, T. L. *Organometallics* **1984**, *3*, 29. (b) Top, S.; Gunn, M.; Jaouen, G.; Vaissermann, J.; Daran, J. C.; McGlinchey, M. J. *Organometallics* **1992**, *11*, 1201. (c) Cao, D. H.; Stang, P. J.; Arif, A. M. *Organometallics* **1995**, *14*, 2733. (d) Bruce, M. I.; Low, P. J.; Skelton, B. W.; White, A. H. *J. Organomet. Chem.* **1996**, *515*, 65. (e) Wu, H.-L.; Lu, G.-L.; Chi, Y.; Farrugia, L. J.; Peng, S.-M.; Lee, G.-H. *Inorg. Chem.* **1996**, *35*, 6015. (f) Schaverien, C. J. *Organometallics* **1994**, *13*, 69. (g) Top, S.; Gunn, M.; Jaouen, G.; Vaissermann, J.; Daran, J. C.; Thornback, J. R. *J. Organomet. Chem.* **1991**, *414*, C22.

(15) Kaesz, H. D.; Saillant, R. B. *Chem. Rev.* **1972**, *72*, 231. See also ref 5h.

Table 1. ^{31}P and ^1H NMR Data^a

	^{31}P	^1H					
		$\delta(\text{H})$	$^2J_{\text{H-P}(1)(\text{trans})}$	$^2J_{\text{H-P}(2)(\text{cis})}$	$^1J_{\text{Pt-H}}$	$^1J_{\text{Pt-H}}$	δ (other)
1b^b	29.21 (P(1), $^1J_{\text{Pt}(1)-\text{P}(1)} = 3843$, $J_{\text{Pt}(2)-\text{P}(1)} = 101$) 11.30 (P(2), $^1J_{\text{Pt}(2)-\text{P}(2)} = 3590$, $J_{\text{Pt}(1)-\text{P}(2)} = 30$) $J_{\text{P}(1)-\text{P}(2)} \approx 0$	-7.44	74.2	14.5	562	515	7.63–7.21 (m, 35H, Ph)
2a^c	17.77 (P(A), $^d 1J_{\text{Pt}(1)-\text{P}(A)} = 2573$) 12.22 (P(B), $^1J_{\text{Pt}(1)-\text{P}(B)} = 2553$, $J_{\text{Pt}(2)-\text{P}(B)} = 166.4$) $^2J_{\text{P}(A)-\text{P}(B)} = 386.2$	-10.75 ^e				535	8.15, 7.5 (m, 30H, Ph) ^f
2c^b	18.23 ($^1J_{\text{Pt-P}} = 3825$, $^2J_{\text{Pt-P}} = 112$)	-8.32 ^g				623	7.33, 7.07 (m, 30H, Ph)
3b^h	17.34 (P(1), $^1J_{\text{Pt}(1)-\text{P}(1)} = 3859$, $J_{\text{Pt}(2)-\text{P}(1)} = 94.9$) 11.96 (P(2), $^1J_{\text{Pt}(2)-\text{P}(2)} = 4403$, $J_{\text{Pt}(1)-\text{P}(2)}$) ⁱ	-9.33	81.7	<i>i</i>	642	566	7.54–7.27 (m, 30H, Ph)
3c^h	10.6 ($^1J_{\text{Pt-P}} = 4513$, $^2J_{\text{Pt-P}}$) ^j	-10.84 ^g				575	7.29, 7.06 (m, 30H, Ph)
4b	16.10 (P(1), $^1J_{\text{Pt}(1)-\text{P}(1)} = 3609$, $J_{\text{Pt}(2)-\text{P}(1)} = 98.2$) 15.55 (P(2), $^1J_{\text{Pt}(2)-\text{P}(2)} = 4151$, $J_{\text{Pt}(1)-\text{P}(2)}$) ^j	-9.9 ^j	75.2	<i>i</i>		592	1.88 (m, 6H), 1.6 (m, 6H) (CH ₂ , PET ₃); 1.08 (m, 9H), 0.95 (m, 9H) (CH ₃ , PET ₃)
4c^k	13.75 ($^1J_{\text{Pt-P}} = 4085$, $^2J_{\text{Pt-P}} = 23.3$)	-11.96 ^g				590	
5	8.48 ($^1J_{\text{Pt-P}} = 4491$, $^4J_{\text{Pt-P}}$) ⁱ						

^a In CDCl₃; *J* in Hz. ^b The same spectral pattern is observed both at -50 °C and in CD₃COCD₃. ^c In HDA. ^d $J_{\text{Pt}(2)-\text{P}(A)}$ not resolved. ^e Quintuplet (1:8:18:8:1), the same pattern is observed at -85 °C. ^f Data at -85 °C: δ 8.66, 8.43, 8.23, 8.1, 7.85, 7.55, 7.47, 7.19, 6.32 (all broad). ^g Quintuplet (1:8:18:8:1). ^h The same spectra (^1H and ^{31}P) are observed at -50 °C. ⁱ Not resolved. ^j Quintuplet of doublets. ^k Data from a mixture of **4b** and **4c** (2:1) in CD₃COCD₃; in CDCl₃ $\delta(\text{P})$ 11.86, $^1J_{\text{Pt-P}} = 4169$ Hz, $\delta(\text{H})$ -12.09, $^1J_{\text{Pt-H}} = 583$ Hz.

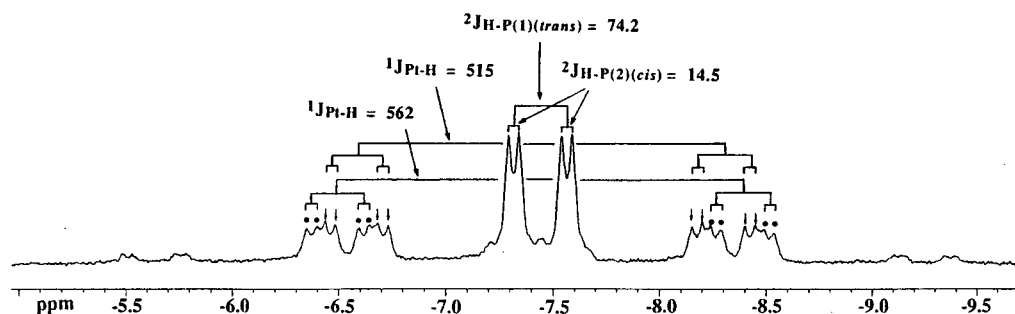


Figure 1. High-field region of the ^1H NMR spectrum of $[\text{trans}-(\text{C}_6\text{F}_5)(\text{PPh}_3)\text{Pt}(\mu\text{-H})(\mu\text{-C}\equiv\text{CPh})\text{Pt}(\text{C}_6\text{F}_5)(\text{PPh}_3)]$ (**1b**) in CDCl₃ at 20 °C; *J* values are in hertz.

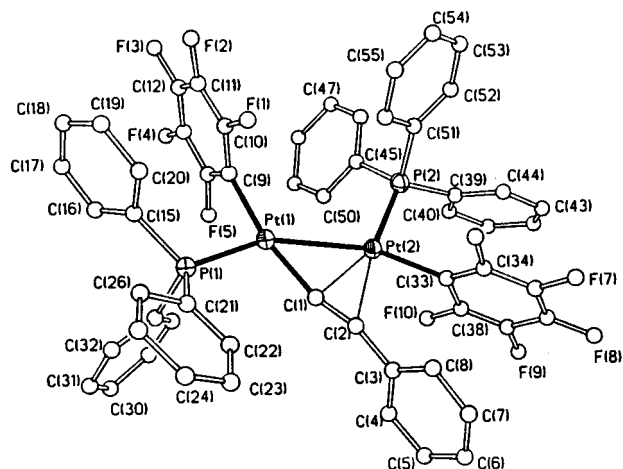


Figure 2. Drawing of the crystal structure of $[\text{trans}-(\text{C}_6\text{F}_5)(\text{PPh}_3)\text{Pt}(\mu\text{-H})(\mu\text{-C}\equiv\text{CH})\text{Pt}(\text{C}_6\text{F}_5)(\text{PPh}_3)]$ (**1b**), showing the atom-labeling scheme.

more acute than that observed in $[\text{Pt}(\mu(\sigma)\text{-}\eta^2\text{-C}\equiv\text{CPh})(\text{C}_6\text{F}_5)(\text{PPh}_3)]_2$ (112.5(2)°). The acetylenic fragment deviates from linearity (angles at C_α and C_β ~163°), adopting a *trans*-bent arrangement. The C(1)–C(2) and Pt(1)–Pt(2) vectors form an angle of 35.77(3)°, but the Pt(1)–Pt(2)–C(1)–C(2) core is roughly planar and the

Table 2. Selected Bond Lengths (Å) and Angles (deg) for $[\text{trans}-(\text{C}_6\text{F}_5)(\text{PPh}_3)\text{Pt}(\mu\text{-H})(\mu\text{-C}\equiv\text{CH})\text{Pt}(\text{C}_6\text{F}_5)(\text{PPh}_3)]$ (**1b**)

Pt(1)–C(1)	1.98(2)	Pt(1)–C(9)	2.08(2)
Pt(1)–P(1)	2.262(3)	Pt(1)–Pt(2)	2.8159(10)
Pt(2)–C(33)	2.048(13)	Pt(2)–C(1)	2.232(13)
Pt(2)–P(2)	2.247(4)	Pt(2)–C(2)	2.354(12)
C(1)–C(2)	1.23(2)	C(2)–C(3)	1.44(2)
C(1)–Pt(1)–C(9)	166.9(5)	C(1)–Pt(1)–P(1)	101.2(4)
C(9)–Pt(1)–P(1)	91.9(4)	C(1)–Pt(1)–Pt(2)	52.0(4)
C(9)–Pt(1)–Pt(2)	114.9(4)	P(1)–Pt(1)–Pt(2)	153.23(9)
C(33)–Pt(2)–C(1)	113.8(5)	C(33)–Pt(2)–P(2)	88.7(4)
C(1)–Pt(2)–P(2)	157.3(4)	C(33)–Pt(2)–C(2)	82.9(5)
P(2)–Pt(2)–C(2)	171.5(3)	C(33)–Pt(2)–Pt(1)	157.8(3)
C(1)–Pt(2)–Pt(1)	44.2(4)	P(2)–Pt(2)–Pt(1)	113.08(9)
C(2)–Pt(2)–Pt(1)	75.2(3)	C(2)–C(1)–Pt(1)	163.8(11)
C(2)–C(1)–Pt(2)	80.0(8)	Pt(1)–C(1)–Pt(2)	83.8(5)
C(1)–C(2)–C(3)	163.6(13)		

P atoms of the PPh₃ ligands and the C_{ipso} carbon atoms of the terminal C₆F₅ groups are also contained in this plane. The least-squares coordination planes (Pt(1), C(1), C(9), P(1) for Pt(1) and Pt(2), C(33), P(2), C(1,2) (C(1,2) = midpoint of C(1)–C(2)) for Pt(2)) are almost coplanar, forming a dihedral angle of 3.52(7)°.

Although the hydride has not been located directly from the final difference Fourier map, its position as a bridging ligand between the two platinum atoms and

Table 3. Pt–Pt Distances, Number of Electrons in the Bridge, and Number of Total Electrons in Binuclear Hydrido-Bridged Platinum(II) Complexes

	electrons in the bridge	total electron	Pt(1)–Pt(2) (Å)	ref
$[(\text{PEt}_3)_2\text{PhPt}(\mu\text{-H})\text{PtY}(\text{PEt}_3)_2]^+$	2	30	3.238(1) (Y = Ph) 3.093(1) (Y = H)	4e 4a
$[\text{Pt}(\mu\text{-H})(\text{SiEt}_3)(\text{PEt}_3)_2]$	4	28	2.692(3)	2
$\{[(\text{C}_6\text{F}_5)(\text{PPh}_3)\text{Pt}]_2(\mu\text{-H})(\mu\text{-C}_6\text{F}_5)\}$ (2c)	4	28	2.6742(7)	this work
$[(\text{PEt}_3)_2\text{Pt}(\mu\text{-H})_2\text{PtX}(\text{PEt}_3)_2]^+$	4	30	2.819(1) (X = Ph) 2.826(1) (X = H)	5c 5c
$[(\text{dppe})\text{Pt}(\mu\text{-H})_2\text{PtH}(\text{dppe})]^+$	4	30	2.728(1)	5d
$\{[(\text{C}_6\text{F}_5)(\text{PPh}_3)\text{Pt}]_2(\mu\text{-H})(\mu\text{-C}\equiv\text{CPh})\}$ (1b)	6	30	2.8159(10)	this work
$[(\text{C}_6\text{F}_5)(\text{PPh}_3)\text{Pt}(\mu\text{-H})(\mu\text{-PPh}_3)\text{Pt}(\text{C}_6\text{F}_5)_2]$ (2a)	6	30		this work
$[(\text{C}_6\text{F}_5)(\text{PPh}_3)\text{Pt}(\mu\text{-H})(\mu\text{-Cl})\text{Pt}(\text{C}_6\text{F}_5)(\text{PPh}_3)]$ (3c)	6	30	2.7593(6)	this work
$\{[(\text{PPh}_2\text{POHOPPh}_2)\text{Pt}]_2(\mu\text{-H})(\mu\text{-PPh}_2)\}$	6	30	2.907(1)	8c
$[(\text{PPh}_3)_2\text{Pt}(\mu\text{-H})(\mu\text{-PPh}_2)\text{PtPh}(\text{PPh}_3)]\text{Z}$	6	30	2.885(1) (Z = $\text{HC}(\text{SO}_2\text{CF}_3)_2$) 2.889(3) (Z = BF_4)	8b 8a
$[(\text{dppe})\text{Pt}(\mu\text{-H})(\mu\text{-S})\text{Pt}(\text{dppe})]^+$	6	30	2.912(2) 2.774(1)	9

approximately *trans* to P(1) is quite clear from the NMR spectroscopic data. Moreover, the Pt(1)–Pt(2) vector does not bisect the P–Pt–C_{ipso} angle of the Pt(C₆F₅)(PPh₃) units, which is also consistent with the presence of a bridging H ligand. The Pt(1)–Pt(2)–C(33) (157.8(3)°) and P(1)–Pt(1)–Pt(2) (153.23(9)°) angles are substantially larger than the corresponding Pt(2)–Pt(1)–C(9) (114.9(4)°) and P(2)–Pt(2)–Pt(1) (113.08(9)°) ones, thus reflecting a considerable bending of both P(2)Ph₃ and C₆F₅ (with C(9)) ligands toward the less sterically demanding bridging hydride ligand. The relative value of the long-range platinum–phosphorus coupling observed ($J_{\text{Pt}(2)\text{-P}(1)} = 101$ Hz and $J_{\text{Pt}(1)\text{-P}(2)} \approx 30$ Hz, respectively) can be readily understood on the basis of this structural feature. It is reasonable that P(2) shows smaller long-range coupling to Pt(1) as a result of the considerable deviation of the angle Pt(1)–Pt(2)–P(2) (113.08(9)°) from linearity. Both Pt–P(1,2) bond distances (2.262(3), 2.247(4) Å), which span the range usually observed for Pt^{II}–P bonds,^{12i,13a} are identical within experimental error, even though the corresponding *trans* bridging ligands are different. Thus, in this complex, the two bridging groups ($\mu\text{-H}$ and $\mu\text{-C}_2\text{R}$) seem to exhibit similar *trans* influences. If the $\mu\text{-hydride}$ ligand is treated as a two-electron anionic donor and the alkynyl bridging group is assumed to be a four-electron anionic donor, then the platinum atoms are in the formal oxidation state +2 and the total valence electron count sums to 30 electrons. This implies a three-center–two-electron bond for Pt–H–Pt, which is consistent with the Pt(1)–Pt(2) distance of 2.816(1) Å. Table 3 reports the observed distances in some dinuclear platinum(II) hydride compounds. As can be seen, the Pt–Pt distance in the present compound is significantly shorter than that observed in 30-electron monohydride-bridged diplatinum complexes such as $[(\text{PEt}_3)_2\text{XPt}(\mu\text{-H})\text{PtY}(\text{PEt}_3)_2]^+$ (X = Y = Ph 3.238(1) Å;^{4e} X = Ph, Y = H, 3.093(1) Å^{4a} (Table 3)) and $[\text{Pt}_2(\text{CH}_3)_2(\mu\text{-H})(\mu\text{-dppm})]$ (2.93 Å)^{6b} and is more in line with those reported for dihydride-bridged compounds such as $[(\text{PEt}_3)_2\text{Pt}(\mu\text{-H})_2\text{PtX}(\text{PEt}_3)]^+$ (X = Ph, 2.819(1) Å; X = H, 2.826(1) Å^{5c}) and $[(\text{dppe})\text{Pt}(\mu\text{-H})_2\text{PtH}(\text{dppe})]^+$ (2.728(1) Å) and similar to 30 e[−] diplatinum hydride species in which a mixed bridging system exists (see Table 3). However, the Pt–Pt separation in this complex (**1b**) is considerably longer than those found in $[\text{Pt}(\mu\text{-H})(\text{SiEt}_3)(\text{PEt}_3)_2]$ (2.692(3) Å)² and **2c** (2.6742(7) Å), both with a total valence electron count of 28 e[−]. This structural fact is in accord with recent qualitative molecular orbital calculations, carried

out for systems of this type, which suggest the existence of through-ring metal–metal interactions for 6- or 4-framework-electron count (FEC, number of electrons in the bridging system).¹⁶ Consistent with these theoretical calculations, the platinum–platinum distance in **1b** with FEC = 6 is longer than in $[\text{Pt}(\mu\text{-H})(\text{SiEt}_3)(\text{PEt}_3)_2]$ (Table 3) and **2c** (2.6742(7) Å) both with a framework electron count of 4. As expected, a further lengthening of this Pt···Pt separation is observed in 32-electron diplatinum complexes such as the well-known doubly halide (~3.5 Å)¹⁷ or doubly alkynyl bridged dimers $[\text{Pt}(\mu(\sigma)\text{-}\eta^2\text{-C}\equiv\text{CPh})(\text{C}_6\text{F}_5)(\text{PPh}_3)_2]$ (3.65 Å),^{13a} $[(\text{dppe})\text{Pt}(\mu\text{-C}\equiv\text{CPh})_2\text{Pt}(\text{C}_6\text{F}_5)_2]$ (3.27 Å),¹²ⁱ and $[\text{Pt}(\mu(\sigma)\text{-}\eta^2\text{-C}\equiv\text{CPh})(\text{C}_6\text{F}_5)_2]_2^{2-}$ (3.43 Å) with FEC = 8.¹²ⁱ

Reaction of *cis*-[Pt(C₆F₅)₂(thf)₂] with *trans*-[Pt(C₆F₅)H(PPh₃)₂]. Although the ability of C₆F₅ ligands to act as 3c–2e-bridging ligands between platinum or palladium centers has been reported recently, this group has seldom been seen to act as a bridging ligand. In fact, the only examples reported have been the *anionic* species $[\text{MM}'(\mu\text{-C}_6\text{F}_5)_2(\text{C}_6\text{F}_5)_4]^{2-}$ (M, M' = Pd, Pt)^{12h,18a} and $[\text{Pt}_2(\mu\text{-X})(\mu\text{-C}_6\text{F}_5)(\text{C}_6\text{F}_5)_4]^-$ (X = C₆F₅^{18b} or 1,8-naphthyridine (napy)^{18c}), and it is worth noting that attempts to prepare other palladium or platinum derivatives containing a mixed $\mu\text{-X}\mu\text{-C}_6\text{F}_5$ (X = Cl, Br, I) bridging system have been unsuccessful.^{12h} Bearing this in mind, and with the aim of preparing a dinuclear *neutral* derivative with a mixed $\mu\text{-H}\mu\text{-C}_6\text{F}_5$ bridging system, we investigated the reaction between *cis*-[Pt(C₆F₅)₂(thf)₂] and *trans*-[Pt(C₆F₅)H(PPh₃)₂].

Addition of *cis*-[Pt(C₆F₅)₂(thf)₂] to a colorless solution of *trans*-[Pt(C₆F₅)H(PPh₃)₂] in CHCl₃ at room temperature results in the immediate precipitation of a white microcrystalline solid in 71% yield, *trans,cis*-[(C₆F₅)(PPh₃)Pt(μ-H)(μ(P)-η²-PPh₃)Pt(C₆F₅)₂]·CHCl₃ (**2a**·CHCl₃) (path ii, Scheme 2), which has been characterized by elemental analysis, spectroscopic methods, and X-ray diffraction analysis. Suitable crystals for an X-ray study of complex **2a** were grown by slow diffusion of n-hexane into a dichloromethane solution of **2a** at low tempera-

(16) Aullón, G.; Alemany, P.; Alvarez, S. *J. Organomet. Chem.* **1994**, *478*, 75.

(17) (a) Watkins, S. F. *J. Chem. Soc. A* **1970**, 168. (b) Anderson, G. K.; Cross, R. J.; Manojlovic-Muir, L.; Muir, K. W.; Salomon, T. *J. Organomet. Chem.* **1979**, *170*, 385.

(18) (a) Usón, R.; Forniés, J.; Tomás, M.; Casas, J. M.; Cotton, F. A.; Falvello, L. R.; Llusar, R. *Organometallics* **1988**, *7*, 2279. (b) Usón, R.; Forniés, J.; Tomás, M.; Casas, J. M.; Cotton, F. A.; Falvello, L. R.; Feng, X. *J. Am. Chem. Soc.* **1993**, *115*, 4145. (c) Ara, I.; Casas, J. M.; Forniés, J.; Rueda, A. *J. Inorg. Chem.* **1996**, *35*, 7345.

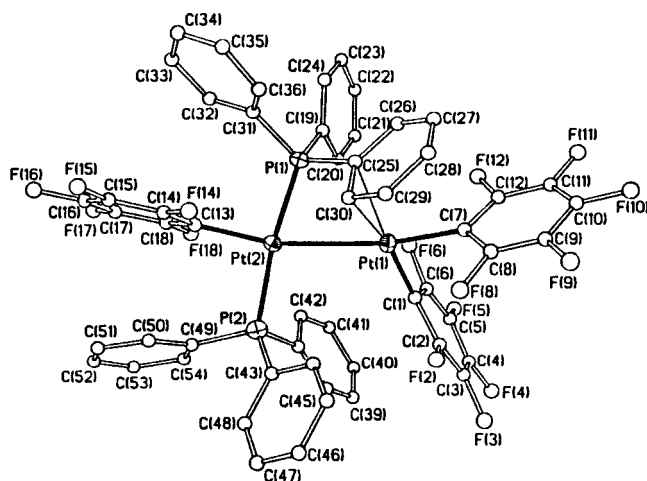
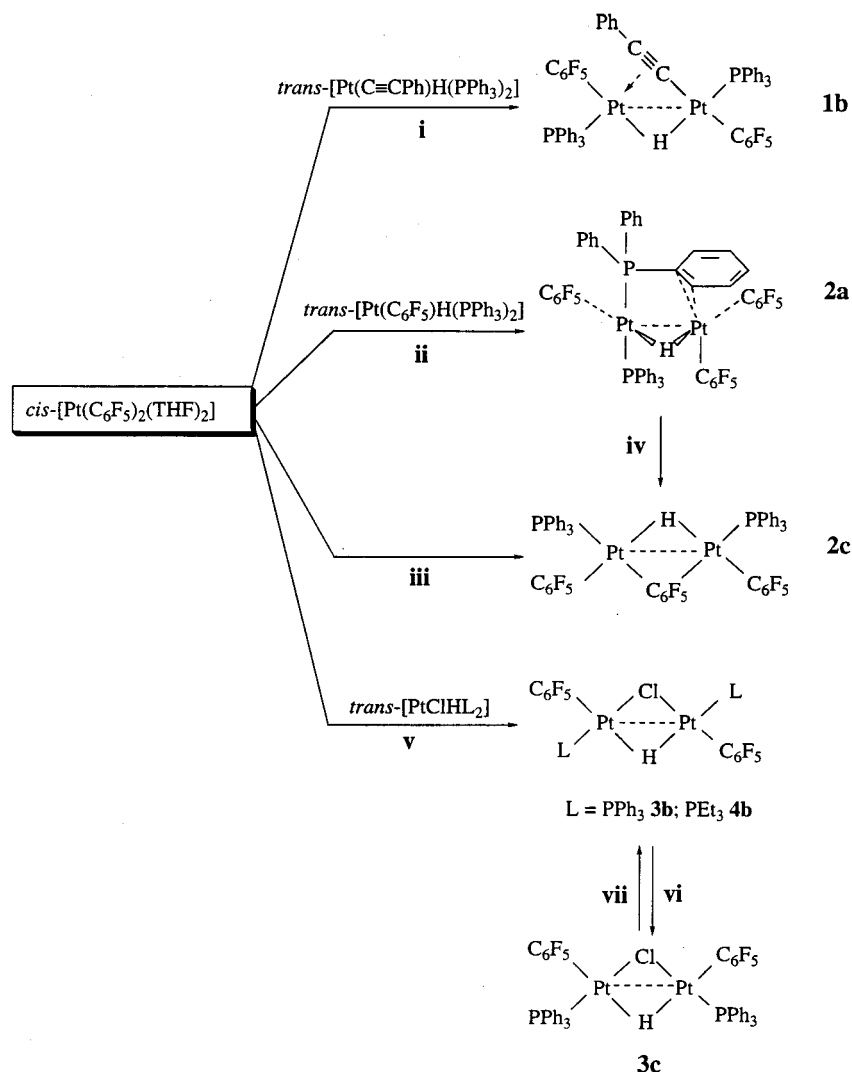
Scheme 2^a

Figure 3. Drawing of the crystal structure of *cis*-[(C₆F₅)₂(PPh₃)Pt(μ-H)(μ-P)-η²-PPh₃]Pt(C₆F₅)₂ (**2a**), showing the atom-labeling scheme.

ture (−40 °C). A drawing of the molecular structure is shown in Figure 3, and selected bond distances and angles are listed in Table 4. It should be noted that the dinuclear complex shows a disorder over two positions related by a pseudo binary axis, affecting the quality of the crystallographic results (see Experimental Section). Despite this fact, the connectivity of the

complex molecule is unambiguously established and the geometric parameters are reasonable.

Clearly, the most interesting feature of this complex is the presence of a triphenylphosphine (P(1)Ph₃) acting as a bridging ligand with P bonded to the Pt(2)C₆F₅P(2)-Ph₃ fragment and η²-bonded *via* the C(25) and C(30) carbon atoms of the C(25–30) phenyl ring to the *cis*-Pt(C₆F₅)₂ fragment. Although the position of the hydride ligand could not be located with certainty, its location as a bridging ligand is confirmed by the ¹H NMR spectrum (see below); it also seems clear from the position of the heavy atoms that could be located *trans* to the carbon atom C(13) bonded to Pt(2) and close to the bisectrix of the P(1)–Pt(2)–P(2) angle (173.0(2)°). The different magnitudes of the C–Pt–Pt angles (C(7)–Pt(1)–Pt(2) = 167.1(4)°; C(13)–Pt(2)–Pt(1) = 157.7(4)°) suggest that the μ-H bridge is slightly asymmetric.

Both the position of the heavy atoms and the inferred position of the hydride indicate that the formation of complex **2a** proceeds with the retention of the original configuration about the platinum centers. Thus, unexpectedly the precursor *trans*-[Pt(C₆F₅)H(PPh₃)₂] acts as a metallo chelating ligand toward the “*cis*-Pt(C₆F₅)₂” fragment. This is in contrast with previous reports, which showed that mononuclear platinum hydride complexes [PtHRL₂] react with coordinatively unsaturated metal fragments L_{*n*}MS, yielding dinuclear de-

Table 4. Selected Bond Lengths (Å) and Angles (deg) for *trans,cis*-[(C₆F₅)₂(PPh₃)₂Pt(μ-H)(μ(P)-η²-PPh₃)Pt(C₆F₅)₂] (2a**)**

Pt(1)–C(1)	1.94(2)	Pt(1)–C(7)	2.01(2)
Pt(1)–C(25)	2.42(2)	Pt(1)–C(30)	2.517(15)
Pt(1)–Pt(2)	2.972(2)	Pt(2)–C(13)	2.02(2)
Pt(2)–P(2)	2.291(4)	Pt(2)–P(1)	2.302(4)
P(1)–C(19)	1.80(2)	P(1)–C(31)	1.81(2)
P(1)–C(25)	1.81(2)	P(2)–C(37)	1.80(2)
P(2)–C(49)	1.81(2)	P(2)–C(43)	1.81(2)
C(25)–C(26)	1.41(2)	C(25)–C(30)	1.42(2)
C(26)–C(27)	1.39(2)	C(27)–C(28)	1.39(3)
C(28)–C(29)	1.37(2)	C(29)–C(30)	1.42(2)
C(1)–Pt(1)–C(7)	87.9(7)	C(1)–Pt(1)–C(25)	167.4(6)
C(7)–Pt(1)–C(25)	92.5(6)	C(1)–Pt(1)–C(30)	159.4(6)
C(7)–Pt(1)–C(30)	91.0(6)	C(1)–Pt(1)–Pt(2)	104.9(5)
C(7)–Pt(1)–Pt(2)	167.1(4)	C(13)–Pt(2)–P(2)	93.9(5)
C(13)–Pt(2)–P(1)	92.7(5)	P(2)–Pt(2)–P(1)	173.0(2)
C(13)–Pt(2)–Pt(1)	157.7(4)	P(2)–Pt(2)–Pt(1)	102.33(13)
P(1)–Pt(2)–Pt(1)	70.74(11)	C(19)–P(1)–C(31)	103.1(7)
C(19)–P(1)–C(25)	107.5(8)	C(31)–P(1)–C(25)	103.3(8)
C(19)–P(1)–Pt(2)	114.0(5)	C(31)–P(1)–Pt(2)	120.9(5)
C(25)–P(1)–Pt(2)	107.0(5)	C(37)–P(2)–C(49)	106.5(8)
C(37)–P(2)–C(43)	106.5(8)	C(49)–P(2)–C(43)	105.3(8)
C(37)–P(2)–Pt(2)	108.0(6)	C(49)–P(2)–Pt(2)	115.9(5)
C(43)–P(2)–Pt(2)	113.9(5)		

rivatives RL₂Pt(μ-H)ML_n stabilized only by a single bridging hydride ligand.^{1a,e,4d–g,o,19} In this case, the presence of two labile solvent molecules in *cis*-[Pt(C₆F₅)₂(thf)₂] and the ability of the “*cis*-Pt(C₆F₅)₂” fragment to stabilize η²-phenyl interactions²⁰ seem to favor the formation of this unusual 1:1 adduct. As far as we know, this is the first crystallographic example characterized with the PPh₃ molecule acting as a μ(P)-η² bridging ligand, though examples of μ(P)-η⁶ PPh₃ ligands have been reported previously.²¹ It is noteworthy that only slight structural differences between the terminal (P(2)Ph₃) and bridging (P(1)Ph₃) triphenylphosphine ligands are observed. Thus, both triphenylphosphine ligands have comparable P–C(phenyl) bond distances (range 1.80(2)–1.81(2) Å) and angles at the phosphorus atoms (range 107.0(5)° for C(25)–P(1)–Pt(2) to 120.9(5)° for C(31)–P(1)–Pt(2)) and the Pt–P distances are identical within experimental error (Pt(2)–P(1) = 2.302(4) Å; Pt(2)–P(2) = 2.291(4) Å). However, as expected, the η² coordination of one phenyl group on P(1) to Pt(2) has a perceptible effect on the P–Pt(2)–Pt(1) angles (P(1)–Pt(2)–Pt(1) = 70.7(1)° versus P(2)–Pt(2)–Pt(1) = 102.3(1)°). The Pt(1)–C distances for this η²-Pt(1) interaction are almost equal within experimental error (Pt(1)–C(25) = 2.42(2) Å, Pt(1)–C(30) = 2.517(15) Å) and are similar to related (η²-aryl)platinum interactions²⁰ and, as expected from the geometry of Pt^{II}–olefin systems, the C(25)–C(30) vector forms an angle of 2.5(1)° with the normal to the Pt(1),C(1),C(7) plane. It should be noted that in spite of the η²-coordination to Pt(1) the phenyl ring C(25)–C(30) remains planar and

(19) (a) Albinati, A.; Demartin, F.; Venanzi, L. M.; Wolfer, M. K. *Angew. Chem., Int. Ed. Engl.* **1988**, *27*, 563. (b) Albinati, A.; Lehner, H.; Venanzi, L. M.; Wolfer, M. *Inorg. Chem.* **1987**, *26*, 3933. (c) McGilligan, B. S.; Venanzi, L. M.; Wolfer, M. *Organometallics* **1987**, *6*, 946. (d) Crespo, M.; Sales, J.; Solans, X. *J. Chem. Soc., Dalton Trans.* **1989**, 1089.

(20) (a) Casas, J. M.; Forniés, J.; Martín, A.; Menjón, B.; Tomás, M. *J. Chem. Soc., Dalton Trans.* **1995**, 2949. (b) Alonso, E.; Forniés, J.; Fortuño, C.; Martín, A.; Orpen, A. G. *J. Chem. Soc., Chem. Commun.* **1996**, 231. (c) Casas, J. M.; Forniés, J.; Martín, A.; Menjón, B. *Organometallics* **1993**, *12*, 4376. (d) Forniés, J.; Menjón, B.; Gómez, N.; Tomás, M. *Organometallics* **1992**, *11*, 1187.

(21) (a) Robertson, G. B.; Whimp, P. O. *J. Organomet. Chem.* **1973**, *60*, C11. (b) Luck, R.; Morris, R. H.; Sawyer, J. F. *Organometallics* **1984**, *3*, 1009.

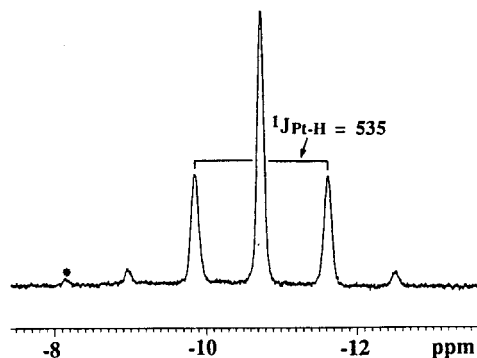


Figure 4. High-field region of the ¹H NMR spectrum of [*trans,cis*-(C₆F₅)₂(PPh₃)₂Pt(μ-H)(μ(P)-η²-PPh₃)Pt(C₆F₅)₂] (**2a**) in CD₃COCD₃ at 20 °C. The signal denoted with an asterisk is due to a small amount of **2c**; *J* is in hertz.

all C–C distances (1.37(2)–1.42(2) Å) and angles within this group are identical within 3σ. This indicates that the loss of aromaticity in the ring upon coordination is negligible, as has been previously suggested in other (η²-aryl)platinum interactions.²⁰ In contrast to complex **1b**, this 1:1 adduct **2a** is not planar and the best least-squares planes around Pt(1) [Pt(1),C(1),C(7) and midpoint of C(25)–C(30)] and Pt(2) (Pt(2),C(13),P(1),P(2)) form a dihedral angle of 35.2(1)°.

Finally, considering the μ-PPh₃ ligand as a four-electron donor, we arrive at a total valence electron count of 30 electrons. This is consistent with the Pt(1)–Pt(2) distance of 2.972(2) Å, which is comparable to those observed in similar diplatinum species (30 e[−]) listed in Table 3.

The NMR data for **2a** in CD₃COCD₃ (Table 1 and Experimental Section) are in keeping with its dinuclear nature. Thus, the ³¹P NMR spectrum confirms the presence of two different PPh₃ groups. It exhibits a central AB quartet (δ[P(A)] 17.77, δ[P(B)] 12.22) with a large coupling constant between the two phosphorus nuclei (²J_{P(A)–P(B)} = 386.2 Hz), surrounded by a pair of AB subspectra (simply “copies” of the central multiplet), the separation of which gives a direct measure of both ¹⁹⁵Pt–P_(A,B) coupling constants [¹J_{Pt–P(A)} = 2573 Hz and ¹J_{Pt–P(B)} = 2553 Hz]. Moreover, the high-field signal (δ 12.22) also exhibits a long-range platinum coupling ²J_{Pt–P(B)} of 166.4 Hz, confirming that, in spite of the use of a donor solvent, the dinuclear structure is retained in solution. The ¹H NMR spectrum at room temperature (see Figure 4) shows in the high-field region a resonance centered at −10.75 ppm (¹J_{Pt(1)–H} ≈ ¹J_{Pt(2)–H} ≈ 535 Hz) with the typical appearance of a bridging hydride ligand: a quintet of relative intensity 1.8:18:8:1 where the signals are separated by ¹/₂J_{Pt–H}. The signals of this quintet are broad, probably due to unresolved coupling to the two mutually *cis* PPh₃ ligands. Only two broad multiplets centered at 8.15 and 7.5 ppm due to PPh₃ ligands are observed in the aromatic region, and the broadness of these resonances led us to examine its spectrum at low temperature. When the system is cooled to −85 °C, a complex pattern with nine broad resonances is observed in the aromatic region. One of them appears clearly shifted to lower frequency (6.32 ppm) and could be tentatively assigned to the *ortho* proton of the phenyl ring involved in the η² interaction, in agreement with similar shifts to higher

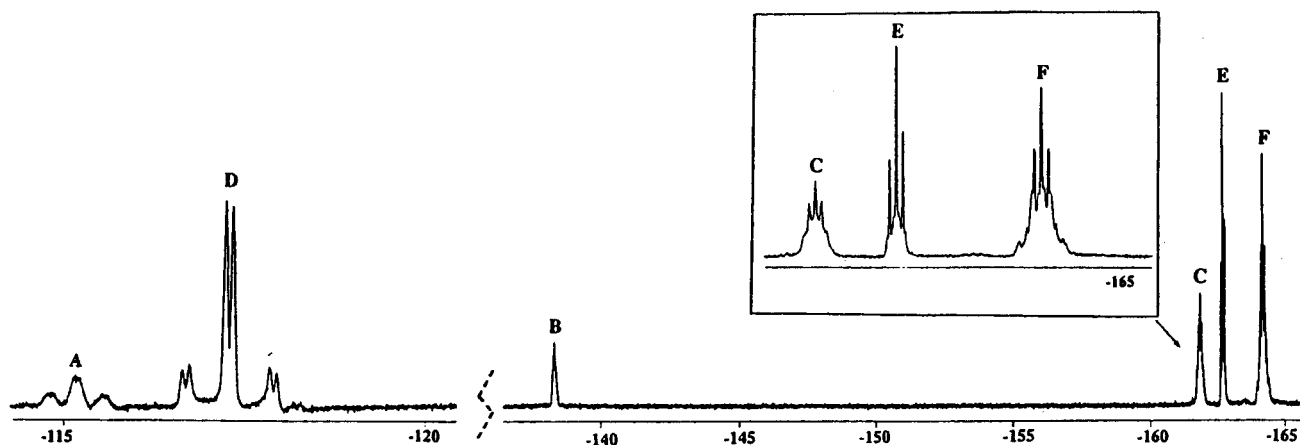


Figure 5. ^{19}F NMR spectrum of $[\text{cis}-(\text{C}_6\text{F}_5)(\text{PPh}_3)\text{Pt}(\mu\text{-H})(\mu\text{-C}_6\text{F}_5)\text{Pt}(\text{C}_6\text{F}_5)(\text{PPh}_3)]$ (**2c**) in CDCl_3 at 20°C .

field observed in other η^2 -aryl interactions.²² However, no ^{195}Pt satellites were observed in any of these signals and we also noted that the hydride region remained essentially unchanged in the temperature range (+15 to -85°C). The ^{19}F NMR spectrum is also temperature-dependent, suggesting the existence of a dynamic process. The ^{19}F NMR spectra registered in the range +15 to -85°C confirm the presence of three nonequivalent C_6F_5 groups. However, for the structure found in the solid state, one would expect to see inequivalence of the *ortho* and *meta* fluorine atoms within each C_6F_5 group. Even at low temperature (-85°C) the spectrum shows the expected two *ortho* and two *meta* fluorine signals for only two of the three C_6F_5 rings (see Experimental Section). Thus, in the *ortho* fluorine region five resonances (-113.1 (d), -113.4 (br), -117.7 (d), -118.0 (d), 118.6 (d)) of relative intensity 1:1:1:1:2 are observed at -85°C , and we tentatively assign the lower frequency signal (-118.6), which remains unchanged at higher temperatures, to the *ortho* fluorine atoms of the C_6F_5 group bonded to Pt(2). The remaining resonances, assigned to the *cis*-Pt(1)(C_6F_5)₂ fragment, suggest that at low temperature the Pt(1) coordination plane does not act as a mirror plane. When the temperature is raised, these four *ortho* fluorine resonances broaden, coalesce at *ca.* -20°C , and finally collapse at room temperature to only one signal centered at -115.4 ppm. A similar behavior is observed for the *meta* fluorine atoms, but for these signals two different *meta* fluorine resonances are observed at room temperature, suggesting that the coincidence of the two *ortho* fluorine atoms on each C_6F_5 ligand is accidental. This pattern suggests that on the NMR time scale a mirror plane is present at room temperature in the fragment Pt(C_6F_5)₂. The simplicity of the aromatic region at room temperature would suggest that the η^2 interaction is lost in solution or at least dynamic exchange of the interaction of Pt(1) with the three phenyl rings on P(1) is easily established. The simplest process that is consistent with these observations and that explains the mirror planes developed on the platinum coordination planes is a rapid inversion of the central dimetallacycle. However, the simple rotation of the C_6F_5 rings about their respective Pt–C bonds cannot be excluded, although this process, as has been noted previously, is

severely hindered in square-planar platinum or palladium complexes.²³

The adduct **2a** is only sparingly soluble in CHCl_3 but on stirring gradually dissolves, yielding a yellow solution; over a period of approximately 28 h at room temperature **2a** completely rearranges to the isomeric derivative *cis*- $[(\text{C}_6\text{F}_5)(\text{PPh}_3)\text{Pt}(\mu\text{-H})(\mu\text{-C}_6\text{F}_5)\text{Pt}(\text{C}_6\text{F}_5)(\text{PPh}_3)]$ (**2c**; Scheme 2). In the conversion of **2a** to **2c** no intermediates were detected by monitoring the isomerization by ^1H and ^{31}P NMR spectroscopy (CDCl_3). It seems, therefore, that the reaction of *cis*- $[\text{Pt}(\text{C}_6\text{F}_5)_2(\text{thf})_2]$ with *trans*- $[\text{Pt}(\text{C}_6\text{F}_5)\text{H}(\text{PPh}_3)_2]$ gives **2a** as the kinetic product, which then transforms into the thermodynamically favored complex **2c**. We note that if the isomerization process is conducted in CD_3COCD_3 , in addition to **2a** and **2c** we always observe the presence (^1H and ^{31}P NMR) of small but at first increasing amounts of *trans*- $[\text{Pt}(\text{C}_6\text{F}_5)\text{H}(\text{PPh}_3)_2]$, which eventually disappears. This fact suggests that **2a** probably dissociates partially in this solvent and that the exchange between free and coordinated $[\text{Pt}(\text{C}_6\text{F}_5)\text{H}(\text{PPh}_3)_2]$ which probably occurs is slow on the NMR time scale. Alternatively, complex **2c** can easily be obtained by refluxing an equimolar mixture of *cis*- $[\text{Pt}(\text{C}_6\text{F}_5)_2(\text{thf})_2]$ and *trans*- $[\text{Pt}(\text{C}_6\text{F}_5)\text{H}(\text{PPh}_3)_2]$ in CHCl_3 for 30 min. Concentration of the resulting deep yellow solution to small volume and addition of *n*-hexane gives **2c** in nearly quantitative yield (92%) as a bright yellow solid (iii, Scheme 2). The NMR data of **2c** indicate that the formation of the expected diplatinum complex with the mixed bridging system Pt($\mu\text{-H})(\mu\text{-C}_6\text{F}_5)\text{Pt}$ has taken place. Thus, the ^1H NMR spectrum shows a diagnostic resonance for $\mu\text{-H}$ at $\delta -8.32$ ($J_{\text{Pt}(1)\text{-H}} \approx J_{\text{Pt}(2)\text{-H}} \approx 623$ Hz, $^2J_{\text{P-H}}$ not resolved) with a pattern similar to that observed for **2a**. The ^{19}F NMR spectrum, which provides additional structural information, is presented in Figure 5. As can be seen, it shows six multiplet signals due to *ortho* (isochronous), and *para* and *meta* fluorine atoms (isochronous) of one bridging (A, B, and C) and two equivalent terminal (D, E, and F) C_6F_5 ligands, as indicated by their relative intensities as well as the relative intensity of the platinum satellites observed for both of the higher frequency signals (*ortho* fluorine region, A and D). The resonances due to the C_6F_5 bridging ligand (-107.15 ppm, $2F_o$; -136.7 ppm, F_p ; -160.6 ppm, $2F_m$) appear at higher frequencies than

(22) Akita, M.; Hua, R.; Oku, T.; Tanaka, M.; Moro-oka, Y. *Organometallics* **1996**, *15*, 4162.

(23) Casares, J. A.; Espinet, P.; Martínez-Ilarduya, J. M.; Lin, Y.-H. *Organometallics* **1997**, *16*, 770 and references therein.

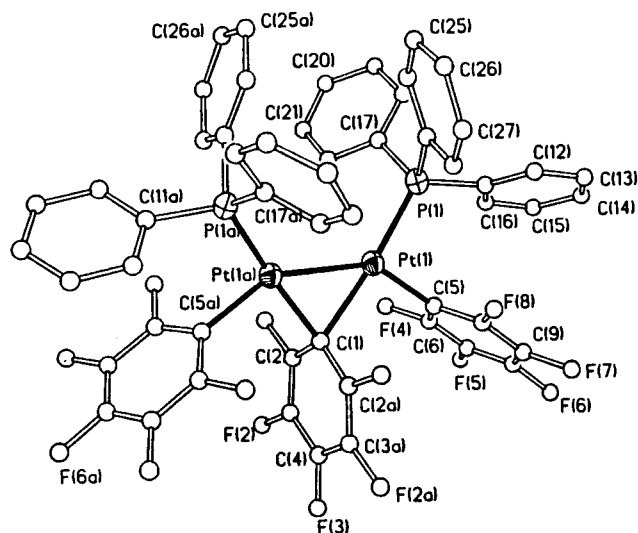


Figure 6. Drawing of the crystal structure of *cis*-[(C₆F₅)(PPh₃)Pt(μ-H)(μ-C₆F₅)Pt(C₆F₅)(PPh₃)] (**2c**), showing the atom-labeling scheme.

Table 5. Selected Bond Lengths (Å) and Angles (deg) for *cis*-[(C₆F₅)(PPh₃)Pt(μ-H)(μ-C₆F₅)Pt(C₆F₅)(PPh₃)] (2c**)^a**

Pt(1)–C(5)	2.033(8)	Pt(1)–C(1)	2.194(8)
Pt(1)–P(1)	2.228(2)	Pt(1)–Pt(1a)	2.6742(7)
C(1)–C(2)	1.383(9)	C(2)–C(3)	1.380(11)
C(3)–C(4)	1.374(10)	C(5)–C(6)	1.373(12)
C(6)–C(7)	1.369(12)	C(7)–C(8)	1.360(2)
C(8)–C(9)	1.305(2)	C(9)–C(10)	1.393(12)
C(5)–Pt(1)–C(1)	91.3(3)	C(5)–Pt(1)–P(1)	91.8(2)
C(1)–Pt(1)–P(1)	173.27(8)	C(5)–Pt(1)–Pt(1a)	143.4(2)
C(1)–Pt(1)–Pt(1a)	52.4(2)	P(1)–Pt(1)–Pt(1a)	124.78(5)
C(2)–C(1)–C(2a)	114.7(10)	C(2)–C(1)–Pt(1a)	111.7(4)
C(2)–C(1)–Pt(1)	119.0(4)	Pt(1a)–C(1)–Pt(1)	75.1(3)
C(10)–C(5)–C(6)	115.4(8)		

^a Symmetry transformation used to generate equivalent atoms: $-x + 3/2, -y, z$.

those of the terminal C₆F₅ groups, in accord with similar observations previously reported for anionic diplatinum derivatives containing bridging and terminal C₆F₅ ligands.^{12h,18} The equivalence of the two terminal C₆F₅ groups in the complex indicates a mutually *cis* disposition in the dinuclear structure. As expected, the two PPh₃ ligands are also equivalent. The ³¹P NMR spectrum exhibits only a singlet signal (δ 18.23, Pt–Pt isotopomer ~44%, A₂ spin system) flanked by platinum satellites due to short-range (¹J_{Pt–P} = 3825 Hz) and long-range (²J_{Pt–P} = 112 Hz) coupling to near and far ¹⁹⁵Pt atoms (¹⁹⁵Pt–Pt and Pt–¹⁹⁵Pt ≈ 45%, AA'X spin systems J_{AA'} = ³J_{P–P'} ≈ 0). Only the most intense signals due to the third isotopomer (¹⁹⁵Pt–¹⁹⁵Pt ≈ 11%, AA'XX' spin system) and separated by $N = {}^1J_{\text{Pt-P}} + {}^2J_{\text{Pt-P}}$ are observed in the spectrum. These lines fall outside the ¹J_{Pt–P} doublet, indicating that ¹J_{Pt–P} and ²J_{Pt–P} are of the same sign.²⁴ Although the two isomers **A** (PPh₃ ligands *trans* to μ-C₆F₅) and **B** (C₆F₅ ligands *trans* to μ-C₆F₅) are compatible with these spectroscopic data, the structure of **2c** (Figure 6, Table 5) was shown to be **A** by X-ray crystallography. The C_{ipso}(C1) and C_{para}(C4) atoms of the C₆F₅ bridging group lie on a crystallographic 2-fold axis, and thus, the two platinum atoms are in identical environments. The dihedral

angles formed by the C₆F₅ rings and the central Pt₂C(1) plane are 89.5(2.7)° (bridging) and 40.55(4)° (terminal). The Pt–C(5) terminal distance (2.033(8) Å) is within the usual range for platinum pentafluorophenyl complexes, and it is shorter than the Pt–C₆F₅ bridging distance (Pt(1)–C(1) = 2.194(8) Å), as previously found for [Pt₂(μ-C₆F₅)₂(C₆F₅)₄]²⁻ ($n = 1, 18b, 218a$). The bond angles around the platinum centers are 91.3(3)° for C(1)–Pt(1)–C(5) and 91.8(2)° for P(1)–Pt(1)–C(5). The Pt–Pt vector does not bisect the PPh₃–Pt–C₆F₅(terminal) fragment; the P(1)–Pt(1)–Pt(1a) angle (124.78(15)°) is less obtuse than C(5)–Pt(1)–Pt(1a) (143.4(2)°), indicating a notable bending of the bulky PPh₃ ligands toward the less demanding hydride bridging ligand, which again was not located in the X-ray study. The Pt(1)–C(1)–Pt(1a) angle is very acute (75.1(3)°), as required by the short Pt(1)–Pt(1a) bond distance of 2.6742(7) Å. This distance is in accord with the presence of two three-center–two-electron bridges between the platinum centers (total valence electron count 28 e⁻) but is clearly shorter than those previously found in the anion [(C₆F₅)₂Pt(μ-C₆F₅)₂–Pt(C₆F₅)₂]²⁻ (2.714(1) Å)^{18a} and in the neutral complex [(PEt₃)(SiEt₃)Pt(μ-H)₂Pt(SiEt₃)(PEt₃)]² (2.692(3) Å), both with similar FEC values of 4.¹⁶

Reaction of *cis*-[Pt(C₆F₅)₂(thf)₂] with *trans*-[PtClHL₂]. Similar dinuclear derivatives containing a mixed chloride–hydride bridging system can also be obtained by treatment of *cis*-[Pt(C₆F₅)₂(thf)₂] with *trans*-[PtClHL₂] (see Scheme 2). Thus, the reactions between *trans*-[PtClHL₂] (L = PPh₃, PEt₃) and *cis*-[Pt(C₆F₅)₂(thf)₂] in CHCl₃ yield almost immediately (1–2 min; NMR spectroscopy) the corresponding *trans* dinuclear isomers [(C₆F₅)₂L₂Pt(μ-H)(μ-Cl)Pt(C₆F₅)₂L] (**3b**, L = PPh₃; **4b**, L = PEt₃). Both complexes are isolated as white solids in high yields (**3b**, 85%; **4b**, 73%) and have been characterized by elemental analyses and spectroscopic methods (see Experimental Section and Table 1). The NMR spectra of **3b** and **4b** are very similar to those observed for compound **1b**, confirming that they are the corresponding *trans* isomers. The ¹⁹F NMR spectra of both compounds show signals corresponding to two nonequivalent C₆F₅ rings, ruling out the alternative *cis* isomers, which should display equivalent C₆F₅ groups. As expected, the ³¹P NMR spectra also display two different singlet resonances (**3b**, 17.34 and 11.96 ppm; **4b**, 16.10 and 15.55 ppm), indicating nonequivalent phosphorus environments. Selective decoupling of the phosphine (but not hydride) protons in their ³¹P NMR spectra split only the downfield signals (17.34 ppm for **3b** and 16.10 ppm for **4b**) into a doublet ($J \approx 83.0$), consistent with hydride ligand *trans* to phosphorus. Therefore, these signals, which exhibit long-range (94.9 Hz, **3b**; 98.2 Hz, **4b**) and short-range (3859 Hz, **3b**; 3609 Hz, **4b**) ¹⁹⁵Pt coupling, are assigned to phosphorus nuclei (P(1)) *trans* to hydride while the resonances at 11.96 ppm (¹J_{Pt(2)–P(2)} = 4403 Hz) for **3b** and at 15.5 ppm ($J_{\text{Pt(2)–P(2)}} = 4151$ Hz) for **4b** are assigned to the phosphine ligands (P(2)) *cis* to H. It is worth mentioning that the ¹J_{Pt–P(1)}} coupling constants (in these derivatives and in complex **1b**) are very large, in agreement with previous observations^{4n,6a,8c} indicating that the μ-H ligands exert a much weaker *trans* influence than do the terminal hydrides. In addition, the presence of a hydride ligand is evidenced by an upfield doublet resonance centered at δ –9.33 for **3b** and at δ –9.9 for}

(24) Kiffen, A. A.; Masters, C.; Visser, J. P. *J. Chem. Soc., Dalton Trans.* **1975**, 1311.

4b with ^{195}Pt satellites ($^1J_{\text{Pt-H}} = 642$ and 566 Hz for **3b** and $^1J_{\text{Pt(1)-H}} \approx ^1J_{\text{Pt(2)-H}} \approx 592$ for **4b**). The doublet structure arises from coupling with the *trans* phosphorus P(1) only ($^2J_{\text{H-P(1)}} = 81.7$ Hz for **3b** and $^2J_{\text{H-P}} = 75.2$ Hz for **4b**), as has been confirmed by the selective decoupling (phosphine protons) ^{31}P NMR experiment mentioned above. In addition to the NMR evidence, the mass spectra of **3b** and **4b** show the expected molecular ion peaks (see Experimental Section), confirming the dinuclear nature of both complexes.

Attempts to obtain crystals of compound **3b** by slow diffusion of *n*-hexane into a CH_2Cl_2 solution of **3b** in the presence of light unexpectedly yield colorless crystals of the *cis* isomer **3c**, which has been characterized by microanalysis and spectroscopic methods and, furthermore, by X-ray crystallography (see below). However, no isomerization is observed if the solution is kept in the dark, suggesting that the isomerization process is probably induced photochemically. This conclusion is further confirmed by the fact that complex **3b** (*trans* isomer) is thermally stable in CHCl_3 at reflux but is quantitatively isomerized to the *cis* isomer (**3c**) upon photolysis (30 min, 125 W, Hg lamp). The isomerization is reversible, and a CDCl_3 solution of **3c** rearranges to a mixture of **3b** and **3c** isomers (2:1 ratio after 10 days at room temperature). We have also observed that the *trans* isomer **3b** slowly transforms into a mixture of the **3b** and **3c** isomers in CD_3COCD_3 . A 2:1 (**3b**/**3c**) ratio has been detected after 8 h, and the mixture remains unchanged after 7 days. It should be noted, however, that prolonged photolysis (14 h, 125 W, Hg lamp) of a solution of complex **3b** yields the dinuclear doubly chloride-bridged complex $[\text{Pt}(\mu\text{-Cl})(\text{C}_6\text{F}_5)(\text{PPh}_3)]_2$ (**5**; $\delta(\text{P})$ 8.48, $J_{\text{Pt-P}} = 4491$ Hz), as characterized by comparison with the NMR spectrum of another sample prepared by treating $[\text{trans-PtCl}_2(\text{PPh}_3)_2]$ with *cis*- $[\text{Pt}(\text{C}_6\text{F}_5)_2(\text{thf})_2]$ (see Experimental Section). A similar behavior is observed in CD_3COCD_3 for complex **4b**, which rearranges into a mixture of **4b** and **4c** (a 2:1 ratio is observed in 2 h). Irradiation of a CH_2Cl_2 solution of **4b** (125 W, Hg lamp) for 30 min also yields a mixture of **4b** and **4c** (ratio 1.2:1) which remains unchanged after 50 min. Due to the similar solubilities of **4b** and **4c** we have not been able to isolate **4c** in pure form, but its spectroscopic data can easily be extracted (^1H and ^{31}P NMR (Table 1), ^{19}F (Experimental Section)) from the NMR spectra of the mixture.

In both of the *cis* dinuclear derivatives, **3c** and **4c**, the resonance due to the hydride bridging ligand is observed as a binomial quintet (couplings to *cis* phosphorus nuclei are not resolved) centered at slightly higher field than that observed for the corresponding *trans* isomers (**3c**, $\delta -10.84$ vs -9.33 for **3b**; **4c**, $\delta -11.96$ vs -9.9 for **4b**). However, the magnitude of the platinum coupling constants ($^1J_{\text{Pt-H}} = 575$ Hz (**3c**), 590 Hz (**4c**)) is comparable to that observed in **3b** and **4b** (see Table 1). The ^{31}P NMR spectra consist, as expected, of a singlet resonance ($\delta(\text{P})$ 10.6 (**3c**), 13.75 (**4c**)) flanked by a single set of short-range-coupling platinum satellites (4513 Hz, **3c**; 4085 Hz, **4c**); the ^{19}F NMR spectra reveal that the two C_6F_5 groups are equivalent (see Experimental Section). Complex **3c** has been characterized by an X-ray crystal structure analysis (Figure 7 and Table 6). The molecule, as anticipated, is a dimer in which the platinum centers are in identical chemical

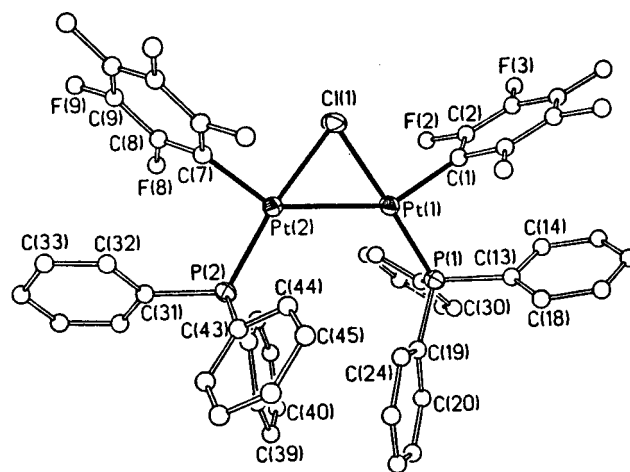


Figure 7. Drawing of the crystal structure of *cis*- $[(\text{C}_6\text{F}_5)(\text{PPh}_3)\text{Pt}(\mu\text{-H})(\mu\text{-Cl})\text{Pt}(\text{C}_6\text{F}_5)(\text{PPh}_3)]$ (**3c**), showing the atom-labeling scheme.

Table 6. Selected Bond Lengths (Å) and Angles (deg) for *cis*- $[(\text{C}_6\text{F}_5)(\text{PPh}_3)\text{Pt}(\mu\text{-H})(\mu\text{-Cl})\text{Pt}(\text{C}_6\text{F}_5)(\text{PPh}_3)]$ (3c**)**

Pt(1)–Pt(2)	2.759(1)	Pt(1)–C(1)	2.005(8)
Pt(1)–P(1)	2.204(2)	Pt(1)–Cl(1)	2.349(2)
Pt(2)–C(7)	2.018(9)	Pt(2)–P(2)	2.197(2)
Pt(2)–Cl(1)	2.342(2)	P(1)–C(19)	1.792(10)
P(1)–C(25)	1.802(10)	P(1)–C(13)	1.821(9)
P(2)–C(37)	1.802(10)	P(2)–C(43)	1.803(9)
P(2)–C(31)	1.805(9)		
C(1)–Pt(1)–P(1)	88.6(2)	C(1)–Pt(1)–Cl(1)	92.(2)
P(1)–Pt(1)–Cl(1)	175.27(9)	C(1)–Pt(1)–Pt(2)	146.6(2)
P(1)–Pt(1)–Pt(2)	124.68(7)	C(7)–Pt(2)–P(2)	95.9(2)
C(7)–Pt(2)–Cl(1)	89.9(2)	P(2)–Pt(2)–Cl(1)	172.52(9)
C(7)–Pt(2)–Pt(1)	143.9(2)	P(2)–Pt(2)–Pt(1)	120.03(7)
Pt(2)–Cl(1)–Pt(1)	72.07(7)		

environments and have mutually *cis* dispositions of both the two C_6F_5 groups and the two PPh_3 ligands. The compound can be described as formed by two distorted-square-planar Pt(II) units having as terminal ligands the C_6F_5 and PPh_3 moieties, with bridging chloride and hydride ligands. Even though it is not possible to locate the hydrogen atom, its bridging position is unequivocally defined by the NMR data (see above). The C(7)Pt(2)P(2) and Pt(1)C(1)P(1) atoms and the bridging Cl(1) atom are essentially in the same plane; the dihedral angle between the platinum coordination planes is only $6.3(2)^\circ$. The P–Pt–Pt angles ($124.68(7)$ and $120.03(7)^\circ$) are similar to those observed in **2c**, indicating a similar bending of the PPh_3 ligands toward the hydride bridging atom.

The bridging chloride ligand is nearly symmetrically bound to both platinum centers, and the Pt–Cl distances (Pt(2)–Cl(1) = $2.342(2)$ Å, Pt(1)–Cl(1) = $2.349(2)$ Å) are comparable to those found in other doubly chloride-bridged diplatinum complexes.²⁵ The Pt–P distances (Pt(2)–P(2) = $2.197(2)$ Å, Pt(1)–P(1) = $2.204(2)$ Å) are significantly shorter than those found in **1b** and **2c**, in keeping with the very low *trans* influence of the chloride bridging ligand.²⁶ The Pt(1)–Cl(1)–Pt(2) angle is very acute ($72.07(7)^\circ$)—notably smaller than those

(25) Kukushkin, V. Y.; Belski, V. K.; Kononov, V. E.; Shifrina, R. R.; Moiseev, A. I.; Vlasova, R. A. *Inorg. Chim. Acta* **1991**, *183*, 57 and references therein.

(26) Appleton, T. G.; Clark, H. C.; Manzer, L. E. *Coord. Chem. Rev.* **1973**, *10*, 335.

found in bis(μ -chloro) complexes^{12p,17,25,27} (*ca.* 96°) but comparable to those found in other dinuclear complexes containing the mixed bridging system μ -Cl, μ -H²⁸ (*ca.* 73°). In accord with this, the platinum–platinum distance is very short (2.7593(6) Å), near the lower end of the range of distances found in related μ -H diplatinum derivatives with a total valence electron count of 30 e⁻ (see Table 3). Notwithstanding, the Pt–Pt distance in this complex with FEC = 6 is, as expected, a bit longer than in **2c** (2.6742(7) Å) or in [Pt(μ -H)-(SiEt₃)(PEt₃)₂]² (2.692(3) Å), both with framework electron counts of 4.

Conclusion

This work provides a simple method for the preparation of a series of diplatinum complexes with unusual μ -H, μ -X (X = C≡CR, C₆F₅, Cl) mixed bridging systems. It has been demonstrated that the overall transformation of *trans*-[Pt(C₆F₅)H(PPh₃)₂] and *cis*-[Pt(C₆F₅)₂(thf)₂] to the thermodynamically more stable dinuclear derivative *cis*-[(C₆F₅)(PPh₃)Pt(μ -H)(μ -C₆F₅)Pt(C₆F₅)(PPh₃)] (**2c**) proceeds through the initial formation of a reasonably stable intermediate, **2a**, which has been shown (X-ray) to contain an unexpected bridging PPh₃ ligand exhibiting a μ (P)- η^2 -phenyl bonding mode. The PPh₃ ligand is a very common 2 e⁻ P-bonded ligand in coordination chemistry. To the best of our knowledge, this is the first example in which this group acts as a four-electron bridging ligand between two metal centers with P bonding to one metal center and η^2 -aryl bonding to the second metal. μ (P)- η^6 -aryl PPh₃ bridging complexes are also a rather rare class of compounds,²¹ though more examples have been reported for η^6 -aryl arene derivatives in which the phosphine is bonded *via* M– π -arene bonds alone without any M–P interactions.²⁹ Examples of fragmentation of P–C bonds on platinum substrates

leading to μ -PPh₂ and often to Pt–phenyl linkages have been reported previously,^{8ab,30} and metalation of a phenyl ring of the PPh₃ ligand has also been observed.³¹ In this context, the structure of **2a** provides an indication that such P–C or C–H bond cleavages could take place *via* the formation of intermediate species in which the PPh₃ behaves as a four-electron ligand by using the P atom and an η^2 -phenyl interaction. Related η^2 -arene–metal interactions are believed to occur prior to C(sp²)–E (E = H, F) bond cleavages.³² It is also worth noting that P–C bond cleavage reactions induced by transition-metal centers have received considerable attention because of their potential role in the deactivation of phosphine-containing homogeneous catalysts.³³

Although no similar adducts have been detected (even at temperatures as low as –50 °C) between the platinum substrates *trans*-[PtHXL₂] (X = C≡CR, Cl) and *cis*-[Pt(C₆F₅)₂(thf)₂], the intermediacy of η^2 -phenyl interactions in the ligand redistribution pathway cannot be ruled out. It is remarkable that these reactions proceed instantaneously, giving the isomeric derivative **1b**, **3b**, or **4b**, and are essentially quantitative. This result is in contrast with the drastic conditions needed in the synthesis, for instance, of dinuclear [Pt(μ -Cl)Cl(PR₃)₂]₂ derivatives, which have been prepared by refluxing [PtCl₂(PR₃)₂] with PtCl₂ in solvents such as xylene/naphthalene,^{34a} tetrachloroethane,^{34b} and *p*-chlorotoluene^{34c} or more recently by refluxing the Zeise dimer [Pt(μ -Cl)Cl(C₂H₄)₂] with the appropriate phosphine in toluene or tetrachloroethane.^{34d} Similar drastic conditions (refluxing toluene, 5 h) are required in the formation of [Pt(μ -Cl)(C₆F₅)(tht)]₂ by reaction of [Pt(C₆F₅)₂(tht)]₂ and PtCl₂.³⁵ It is clear that in all these reactions the formation of the final products necessarily implies the migration of ligands between the two platinum centers. However, even though in the synthesis of the diplatinum complexes **1–4** a precursor much more soluble and reactive than PtCl₂ (*cis*-[Pt(C₆F₅)₂(thf)₂]) is used, the hydride ligand seems to play a prominent role, since the analogous reaction between *trans*-[PtCl₂(PR₃)₂] and *cis*-[Pt(C₆F₅)₂(thf)₂] to give **5** also requires longer reaction times for completion (24 h, reflux).

(27) (a) Goel, A. B.; Goel, S.; Vanderveer, D. *Inorg. Chim. Acta* **1981**, *54*, L267. (b) Albinati, A.; Naegeli, R.; Ostoja, K. H. A.; Pregosin, P. S.; Ruegger, H. *Inorg. Chim. Acta* **1983**, *76*, L231. (c) Clark, H. C.; Ferguson, G.; Goel, A. B.; Ruhl, B. L. *Organometallics* **1984**, *3*, 15. (d) Usón, R.; Forniés, J.; Tomás, M.; Casas, J. M.; Cotton, F. A.; Falvello, L. R. *Inorg. Chem.* **1987**, *26*, 3482. (e) Phillips, I. G.; Ball, R. G.; Cavell, R. G. *Inorg. Chem.* **1988**, *27*, 4038. (f) Alyea, E. C.; Ferguson, G.; Malito, J.; Ruhl, B. L. *Organometallics* **1989**, *8*, 1188. (g) Vila, J. M.; Gayoso, M.; Pereira, M. T.; Romar, A.; Fernández, J. J. *J. Organomet. Chem.* **1991**, *401*, 385. (h) Stang, P.; Huang, Y.-H.; Arif, A. M. *Organometallics* **1992**, *11*, 231. (i) King, S. A.; Engen, D. V.; Fisher, H. E.; Schwartz, J. *Organometallics* **1991**, *10*, 1195. (j) Rashidi, M.; Fakhroei, Z.; Puddephatt, R. J. *J. Organomet. Chem.* **1991**, *406*, 261.

(28) (a) Albinati, A.; Lehner, H.; Venanzi, L. M. *Inorg. Chem.* **1985**, *24*, 1483. (b) Lehner, H.; Matt, D.; Togui, A.; Thouvenot, R.; Venanzi, L. M.; Albinati, A. *Inorg. Chem.* **1984**, *23*, 4254. (c) Churchill, M. R. In *Transition Metal Hydrides*; Bau, R., Ed.; Advances in Chemistry Series 167; American Chemical Society: Washington, DC, 1978; p 36. (d) Robinson, S. D.; Sahajpal, A.; Tocher, D. *J. Chem. Soc., Dalton Trans.* **1995**, 3497.

(29) Morris, M. J. In *Comprehensive Organometallic Chemistry II*; Abel, E. W.; Stone, F. G. A.; Wilkinson, G., Eds.; Pergamon Press: Oxford, U.K., 1995; Vol. 5, Chapter 8, p 529.

(30) (a) Taylor, N. J.; Chieh, P. C.; Carty, A. *J. Chem. Soc., Chem. Commun.* **1975**, 448. (b) Gillar, R. D.; Ugo, R.; Cariati, F.; Cenini, S.; Bonati, F. *Chem. Commun.* **1966**, 869. (c) Ugo, R.; La Monica, G.; Cariati, F.; Cenini, S.; Conti, F. *Inorg. Chim. Acta* **1970**, *4*, 390. (d) Ugo, R.; Cenini, S.; Pilbrow, M.; Deibl, B.; Scheider, G. *Inorg. Chim. Acta* **1976**, *18*, 113. (e) Blake, D. M.; Nyman, C. J. *J. Chem. Soc., Dalton Trans.* **1969**, 483. (f) Blake, D. M.; Nyman, C. J. *J. Am. Chem. Soc.* **1970**, *92*, 5359. (g) Tolman, C. A.; Seidel, W. C.; Gerlach, D. H. *J. Am. Chem. Soc.* **1972**, *94*, 2669. (h) Durkin, T. P.; Schram, E. P. *Inorg. Chem.* **1972**, *11*, 1048, 1054. (i) Glockling, F.; McBride, T.; Pollock, R. J. *J. Chem. Soc., Chem. Commun.* **1973**, 650. (j) Evans, D. G.; Hughes, G. R.; Mingos, D. M. P.; Bassett, J.-M.; Welch, A. J. *J. Chem. Soc., Chem. Commun.* **1980**, 1255. (k) Bender, R.; Braunstein, P.; Dedieu, A.; Ellis, P. D.; Huggins, B.; Harvey, P. D.; Sappa, E.; Tiripichio, A. *Inorg. Chem.* **1996**, *35*, 1223.

(31) (a) Clark, H. C.; Hine, K. E. *J. Organomet. Chem.* **1976**, *105*, C32. (b) Rice, N. C.; Oliver, J. D. *J. Organomet. Chem.* **1978**, *145*, 121. (c) Bennett, M. A.; Perry, D. E.; Bhargava, S. K.; Ditzel, E. J.; Robertson, G. B.; Willis, A.-C. *J. Chem. Soc., Chem. Commun.* **1987**, 1613. (d) Cauty, A. J.; Minchin, N. J.; Patrick, J. M.; White, A. H. *J. Chem. Soc., Dalton Trans.* **1983**, 1253. (e) Scheffknecht, C.; Rhomberg, A.; Müller, E. P.; Peringer, P. *J. Organomet. Chem.* **1993**, *463*, 245. (f) Chakravarty, A. R.; Cotton, F. A.; Tocher, D. A. *Inorg. Chem.* **1984**, *23*, 4697. (g) Chakravarty, A. R.; Cotton, F. A.; Tocher, D. A. *Organometallics* **1985**, *4*, 8. (h) Janowicz, A. H.; Bergman, R. G. *J. Am. Chem. Soc.* **1983**, *105*, 3929. (i) Cole-Hamilton, D. J.; Wilkinson, G. *J. Chem. Soc., Dalton Trans.* **1979**, 1283; **1977**, 797. (j) Cole-Hamilton, D. J.; Wilkinson, G. *Nouv. J. Chim.* **1977**, *1*, 141. (k) Werner, H.; Gotzig, J. *J. Organomet. Chem.* **1985**, *284*, 73.

(32) (a) Jones, W. D.; Feher, F. J. *Acc. Chem. Res.* **1989**, *22*, 91; *J. Am. Chem. Soc.* **1986**, *108*, 4814; **1984**, *106*, 1650; **1982**, *104*, 4240. (b) Griffiths, D. C.; Young, G. B. *Organometallics* **1989**, *8*, 875 and references therein. (c) Faller, J. W.; Smart, C. J. *Organometallics* **1989**, *8*, 602. (d) Stoutland, P. O.; Bergman, R. G. *J. Am. Chem. Soc.* **1988**, *110*, 5732. (e) Lin, C.-H.; Li, C.-S.; Cheng, C.-H. *Organometallics* **1994**, *13*, 18. (f) Belt, S. T.; Dong, L.; Duckett, S. B.; Jones, W. D.; Partridge, M. G.; Perutz, R. N. *J. Chem. Soc., Chem. Commun.* **1991**, 266. (g) Jones, W. D.; Partridge, M. G.; Perutz, R. N. *J. Chem. Soc., Chem. Commun.* **1991**, 264. See also references given in ref 12b–d.

(33) (a) Garrou, P. E. *Chem. Rev.* **1985**, *85*, 171. (b) Dubois, R. A.; Garrou, P. E. *Organometallics* **1986**, *5*, 466.

(34) (a) Goodfellow, R. J.; Venanzi, L. M. *J. Chem. Soc.* **1965**, 7533. (b) Smithies, A. C.; Schmidt, P.; Orchin, M. *Inorg. Synth.* **1970**, *12*, 240. (c) Baratta, W.; Pregosin, P. *Organomet. Chem. Acta* **1993**, *209*, 85. (d) Boag, N. M.; Ravetz, M. S. *J. Chem. Soc., Dalton Trans.* **1995**, 3473.

(35) Usón, R.; Forniés, J.; Espinet, P.; Alfranca, G. *Synth. React. Inorg. Met.-Org. Chem.* **1980**, *10*, 579.

Experimental Section

General Methods. All reactions were carried out under N_2 using dried solvents purified by known procedures and distilled prior to use. IR spectra were recorded on a Perkin-Elmer 883 spectrometer from Nujol mulls between polyethylene sheets. NMR spectra were recorded on a Bruker ARX 300 spectrometer. Chemical shifts are reported in ppm relative to external standards ($SiMe_4$, $CFCl_3$, and 85% H_3PO_4). Elemental analyses were carried out with a Perkin-Elmer 240C microanalyzer and the mass spectra on a VG Autospec spectrometer. The starting complexes *trans*-[PtXHL₂] (L = PPh₃, X = C≡CPh,^{36a} C₆F₅,^{36b} Cl;^{36c} L = PEt₃, X = Cl^{36d}), *trans*-[PtCl₂(PPh₃)₂],³⁷ and *cis*-[Pt(C₆F₅)₂(thf)₂]¹¹ were prepared as described elsewhere.

Preparation of *trans*-[(C₆F₅)(PPh₃)Pt(μ-H)(μ-C≡CPh)-Pt(C₆F₅)(PPh₃)] (1b). To a CHCl₃ solution (20 mL) of *trans*-[Pt(C≡CPh)H(PPh₃)₂] (0.113 g, 0.138 mmol) was added *cis*-[Pt(C₆F₅)₂(thf)₂] (0.093 g, 0.138 mmol), and the mixture was stirred at room temperature for 1 h. The resulting solution was evaporated to dryness, and the residue was treated with methanol, yielding **1b** (yield 75%) as a white solid. Anal. Calcd for C₅₆H₃₆P₂F₁₀Pt₂: C, 49.79; H, 2.69. Found: C, 49.48; H, 2.87. EI-MS (FAB⁺): molecular peak not observed, *m/z* 1081 ([Pt₂(C₆F₅)(PPh₃)₂]⁺, 15%), 719 ([Pt(PPh₃)₂]⁺, 35%), 528 ([Pt(C₆F₅)₂]⁺, 47%), 456 ([Pt(PPh₃)₂]⁺, 55%). IR (cm⁻¹): ν(C≡C) 2018 (w), ν(C₆F₅)_{X-sens} 797 (m), 784 (m).³⁸ ¹⁹F NMR (CDCl₃; 20 °C): δ -116.4 (dm, ³J_{Pt-F_o} = 286 Hz, 2F_o), -118.7 (d, ³J_{Pt-F_o} = 345 Hz, 2F_o), -163.5 (m, 1F_p), -164.3 (m, 2F_m), -164.7 (t, 1F_p), -165.3 (m, 2F_m). The same spectral pattern was observed at -50 °C. ¹³C NMR (CDCl₃, -50 °C): δ 147.2-137.3 (C₆F₅), 134.1 (d, J_{C-P} = 11.8 Hz), 133.6 (d, J_{C-P} = 11.2 Hz) (C_o, PPh₃), 131.0, 130.9 (C_p, PPh₃), 130.1 (d, J_{C-P} = 61 Hz), 129.1 (d, J_{C-P} = 65 Hz) (C_i, PPh₃), 128.8, 128.6 (s, Ph), 127.8 (m, C_m, PPh₃), 127.4 (s, Ph), 124.9 (d, J_{C-P} = 3.3 Hz, tentatively assigned to C_β, C_α≡C_βPh), 108.7 (d, J_{C-P} = 21.7 Hz, C_α, C_α≡C_βPh) (¹⁹⁵Pt satellites not observed).

Preparation of *trans,cis*-[(C₆F₅)(PPh₃)Pt(μ-H)(μ(P)-η²-PPh₃)Pt(C₆F₅)₂] (2a). To a colorless solution of *trans*-[Pt(C₆F₅)H(PPh₃)₂] (0.150 g, 0.169 mmol) in CHCl₃ (5 mL) was added *cis*-[Pt(C₆F₅)₂(thf)₂] (0.114 g, 0.169 mmol), immediately giving a pale yellow solution. After a few (1-2) minutes of stirring a white solid precipitates. The mixture was stirred for 30 min, and then the resulting white microcrystalline solid (2a·CHCl₃) was filtered off; yield 71%. Anal. Calcd for C₅₅H₃₂F₁₅Cl₃P₂Pt₂: C, 43.00; H, 2.03. Found: C, 43.20; H, 2.08. EI-MS (FAB⁺): molecular peak not observed, *m/z* 1082 ([M - 2C₆F₅]⁺, 20%), 1005 ([Pt₂(C₆F₅)(PPh₂)(PPh₃)₂]⁺, 28%), 888 ([Pt(C₆F₅)H(PPh₃)₂]⁺, 40%), 720 ([PtH(PPh₃)₂]⁺, 85%), 529 ([Pt(C₆F₅)₂]⁺, 21%), 456 ([Pt(PPh₃)₂]⁺, 68%), 378 ([Pt(PPh₂) - 2H]⁺, 88%). IR (cm⁻¹): ν(C₆F₅)_{X-sens} 804 (s), 793 (vs). ¹⁹F NMR (CD₃COCD₃; 20 °C) δ -115.4 (s, br, 4F_o, ³J_{Pt-F_o} ≈ 408 Hz), -117.7 (d, 2F_o, ³J_{Pt-F_o} ≈ 326 Hz), -162.97, -163.05 (overlapping of two t, 2F_p), -163.2 (t, 1F_p), -163.7 (m, 2F_m), -164.8 (m, 2F_m), -165.8 (m, 2F_m). ¹⁹F NMR (CD₃COCD₃; -85 °C): δ -113.1 (d, 1F_o, ³J_{Pt-F_o} ≈ 477 Hz), -113.4 (s, br, 1F_o, ³J_{Pt-F_o} ≈ 363 Hz), -117.7 (d, 1F_o), -118.0 (d, 1F_o), -118.6 (d, 2F_o, ³J_{Pt-F_o} ≈ 296 Hz), -161.8 (m, 3F_p), -162.7 (m, 1F_m), -163.2 (m, 2F_m), -164.1 (m, 1F_m), -165.0 (m, 2F_m). The ¹³C NMR spectrum could not be recorded due to the low solubility of the complex.

Preparation of *cis*-[(C₆F₅)(PPh₃)Pt(μ-H)(μ-C₆F₅)Pt(C₆F₅)(PPh₃)] (2c). To a solution of *cis*-[Pt(C₆F₅)₂(thf)₂] (0.200 g, 0.297 mmol) in CHCl₃ (30 mL) was added *trans*-[Pt(C₆F₅)H(PPh₃)₂] (0.262 g, 0.297 mmol). The mixture was refluxed for 30 min, and the colorless solution gradually turned deep

yellow. Concentration of the solution to small volume (~2 mL) and treatment with *n*-hexane afforded **2c** as a bright yellow solid; yield 92%. Anal. Calcd for C₅₄H₃₁F₁₅P₂Pt₂: C, 45.77; H, 2.21. Found: C, 45.72; H, 2.20. EI-MS (FAB⁺): molecular peak not observed, *m/z* 1081 ([M - 2C₆F₅]⁺, 51%), 1004 ([Pt₂(C₆F₅)(PPh₂)(PPh₃)₂]⁺, 100%), 529 ([Pt(C₆F₅)₂]⁺, 29%), 456 ([Pt(PPh₃)₂]⁺, 65%), 378 ([Pt(PPh₂) - 2H]⁺, 79%). IR (cm⁻¹): ν(C₆F₅)_{X-sens} 795 (vs, br). ¹⁹F NMR (CDCl₃; at 20 °C): δ -107.15 (s, br, 2F_o, ³J_{Pt-F_o} = 217 Hz, C₆F₅ bridging) -118.0 (d, 4F_o, ³J_{Pt-F_o} = 335 Hz, C₆F₅ terminal) -136.7 (1F_p, C₆F₅ bridging) -160.6 (m, 2F_m, C₆F₅ bridging), -161.5 (t, 2F_p, C₆F₅ terminal), -163.5 (m, 4F_m, C₆F₅ terminal). The same spectral pattern is observed at -50 °C. ¹³C NMR (CDCl₃; 20 °C): δ 158.7 (br), 155.3 (br), 147.5 (br), 144.1 (br), 138.4 (br), 138 (br), (C₆F₅), 133.6 (m, C_o, Ph), 130.7 (s, C_p, Ph), 129.6 (d, C_i, J_{P-C} = 62 Hz, Ph), 127.8 (m, C_m, Ph).

Preparation of *trans*-[(C₆F₅)(PPh₃)Pt(μ-H)(μ-Cl)Pt(C₆F₅)(PPh₃)] (3b). *cis*-[Pt(C₆F₅)₂(thf)₂] (0.178 g, 0.264 mmol) was added to a solution of *trans*-[PtClH(PPh₃)₂] (0.200 g, 0.264 mmol) in CHCl₃ (10 mL). The mixture was stirred for 10 min, and then the solution was evaporated to dryness. Addition of methanol (5 mL) caused the separation of **3b** as a white solid (85% yield). Anal. Calcd for C₄₈H₃₁F₁₀P₂ClPt₂: C, 44.85; H, 2.43. Found: C, 45.01; H, 2.46. EI-MS (FAB⁺): *m/z* 1283 ([M - H]⁺, 3%), 1081 ([M - H - Cl - C₆F₅]⁺, 15%), 719 ([Pt(PPh₃)₂]⁺, 17%), 528 ([Pt(C₆F₅)₂], 25%), 456 ([Pt(PPh₃)], 82%), 378 ([PtPPh₂ - 2H], 100%). IR (cm⁻¹): ν(C₆F₅)_{X-sens} 806 (vs), 795 (s), ν(Pt-Cl) 320 (m with sh). ¹⁹F NMR (CDCl₃; 20 °C): δ -117.4 (d, 2F_o, ³J_{Pt-F_o} = 339 Hz) -118.3 (d, 2F_o, ³J_{Pt-F_o} = 412 Hz), -161.3 (t, F_p), -163.5 (t, F_p), -163.9 (m, 2F_m), -164.9 (m, 2F_m). The same pattern is observed at -50 °C. ¹³C NMR (CDCl₃): δ 148.6-134.8 (br, C₆F₅), 133.9 (d, ²J_{P-C} = 11.5 Hz), 133.5 (d, ²J_{P-C} = 11.31 Hz) (C_o, Ph, PPh₃), 130.96, 130.94 (C_p, Ph, PPh₃), 129.1 (d, ¹J_{P-C} = 67.3 Hz), 128.9 (d, ¹J_{P-C} = 60.9) (C_{ipso}, Ph, PPh₃), 127.9 (m, C_m, Ph, PPh₃).

Preparation of *cis*-[(C₆F₅)(PPh₃)Pt(μ-H)(μ-Cl)Pt(C₆F₅)(PPh₃)] (3c). **Method i.** Colorless crystals of **3c** (30 mg) are obtained by slow diffusion (15 days) of *n*-hexane into a CH₂Cl₂ solution of **3b** (50 mg) at room temperature in the presence of sunlight. We note that, if the mixture is kept in the freezer, only crystals of **3b** are obtained.

Method ii. A solution of **3b** (0.12 g, 0.09 mmol) in CH₂Cl₂ (150 mL) was irradiated through Pyrex glass, at room temperature under an argon atmosphere, using a medium-pressure mercury lamp (125 W) for 30 min until the complete transformation of starting product (monitored by ³¹P and ¹H NMR). The solution was evaporated under reduced pressure to small volume and was treated with hexane, giving pure **3c** as a white solid (80% yield). Anal. Calcd for C₄₈H₃₁F₁₀P₂-ClPt₂: C, 44.85; H, 2.43. Found: C, 45.10; H, 2.63. EI-MS (FAB⁺): *m/z* 1283 ([M - H]⁺, 7%), 1081 ([M - H - Cl - C₆F₅]⁺, 17%), 719 ([Pt(PPh₃)₂]⁺, 15%), 528 ([Pt(C₆F₅)₂]⁺, 25%), 456 ([PtPPh₃]⁺, 75%), 378 ([Pt(PPh₂) - 2H]⁺, 100%). IR (cm⁻¹): ν(C₆F₅)_{X-sens} 806 (vs), 798 (vs), ν(Pt-Cl) 316 (s). ¹⁹F NMR (CDCl₃; 20 °C): δ -117.7 (d, F_o, ³J_{Pt-F_o} = 323 Hz), -161.3 (t, F_p), -163.9 (m, F_m). The same pattern is observed at -50 °C.

Preparation of *trans*-[(C₆F₅)(PEt₃)Pt(μ-H)(μ-Cl)Pt(C₆F₅)(PEt₃)] (4b). Complex **4b** is obtained in a similar way to complex **3b**, with *trans*-[PtClH(PEt₃)₂] (0.139 g, 0.297 mmol) and *cis*-[Pt(C₆F₅)₂(thf)₂] (0.200 g, 0.297 mmol) as starting materials; yield 72%. Anal. Calcd for C₂₄H₃₁F₁₀P₂ClPt₂: C, 28.91; H, 3.03. Found: C, 28.91; H, 3.00. EI-MS (FAB⁺): *m/z* 995 ([M - 2H]⁺, 20%), 829 ([M - C₆F₅]⁺, 30%). IR (cm⁻¹): ν(C₆F₅)_{X-sens} 805 (vs), 792 (s), ν(Pt-Cl) 305 (m). ¹⁹F NMR (CDCl₃): δ -117.3 (d, 2F_o, ³J_{Pt-F_o} = 354 Hz), -117.7 (d, 2F_o, ³J_{Pt-F_o} = 447 Hz), -160.2 (t, F_p), -161.2 (t, F_p), -163.2 (m, 2F_m), -163.7 (m, 2F_m).

Mixture of 4b and 4c. A solution of **4b** (0.100 g, 0.100 mmol) in CH₂Cl₂ (150 mL) was irradiated through Pyrex glass, at room temperature under an argon atmosphere, using a medium-pressure mercury lamp (125 W) for 30 min. The NMR spectra of the resulting solution indicates the presence of a

(36) (a) Furlani, A.; Licocchia, S.; Russo, M. V.; Chiesi-Villa, A.; Guastini, C. *J. Chem. Soc., Dalton Trans.* **1982**, 2449. (b) Crespo, M.; Sales, J.; Soláns, X.; Font-Altaba, M. *J. Chem. Soc., Dalton Trans.* **1988**, 1617. (c) Bailar, J. C.; Itatani, H. *Inorg. Chem.* **1965**, 4, 1618. (d) Phillips, J. R.; Trogler, W. C. *Inorg. Synth.* **1992**, 29, 189.

(37) Gavinato, G.; Toniolo, L. *Inorg. Chim. Acta* **1981**, 52, 39.

(38) Maslowsky, E., Jr. *Vibrational Spectra of Organometallic Compounds*; Wiley: New York, 1977; p 437, and references therein.

Table 7. Crystal Data and Structure Refinement Parameters for Complexes 1b, 2a, 2c, and 3c

complex	1b ·0.5CH ₂ Cl ₂	2a ·1.25CH ₂ Cl ₂	2c ·C ₇ H ₈	3c
empirical formula	C ₅₆ H ₃₆ F ₁₀ P ₂ Pt ₂ ·0.5CH ₂ Cl ₂	C ₅₄ H ₃₁ F ₁₅ P ₂ Pt ₂ ·1.25CH ₂ Cl ₂	C ₅₄ H ₃₁ F ₁₅ P ₂ Pt ₂ ·C ₇ H ₈	C ₄₈ H ₃₁ ClF ₁₀ P ₂ Pt ₂
unit cell dimens				
<i>a</i> (Å)	33.589(7)	20.007(3)	17.279(3)	19.717(2)
<i>b</i> (Å)	11.181(2)	13.8247(9)	17.512(4)	17.212(3)
<i>c</i> (Å)	28.843(6)	20.179(3)	18.338(4)	25.108(3)
α (deg)	90	90	90	90
β (deg)	112.10(3)	111.412(15)	90	90
γ (deg)	90	90	90	90
<i>V</i> (Å ³), <i>Z</i>	10 036(4), 8	5196(1), 4	5549(2), 4	8521(2), 8
wavelength (Å)	0.710 73	0.710 73	0.710 73	0.710 73
temp (K)	210(1)	150(1)	210	200(1)
radiation	graphite monochrom Mo K α	graphite monochrom Mo K α	graphite monochrom Mo K α	graphite monochrom Mo K α
cryst syst	monoclinic	monoclinic	orthorhombic	orthorhombic
space group	<i>C2/c</i>	<i>P2₁/c</i>	<i>Pnna</i>	<i>Pbca</i>
cryst dimens (mm)	0.23 × 0.22 × 0.19	0.40 × 0.30 × 0.20	0.51 × 0.26 × 0.24	0.54 × 0.22 × 0.14
abs coeff (mm ⁻¹)	5.820	5.662	5.184	6.777
transmissn factors	0.379, 0.255	0.854, 0.435	0.223, 0.191	0.973, 0.652
abs corr	ψ scans	ψ scans	ψ scans	ψ scans
diffractometer	Siemens STOE/AED2	Enraf Nonius CAD4	Siemens STOE/AED2	Siemens P4
2 θ range (deg)	4–48 (+ <i>h</i> , + <i>k</i> , \pm <i>l</i>)	4–50 (\pm <i>h</i> , + <i>k</i> , + <i>l</i>)	4–50 (+ <i>h</i> , + <i>k</i> , + <i>l</i>)	3.5–52 (+ <i>h</i> , + <i>k</i> , - <i>l</i>)
no. of rflns collected	7782	9417	5410	9805
no. of indep rflns	7571 (<i>R</i> (int) = 0.0503)	9111 (<i>R</i> (int) = 0.0446)	4888 (<i>R</i> (int) = 0.00)	8274 (<i>R</i> (int) = 0.0471)
refinement method	full-matrix least-squares on <i>F</i> ²	full-matrix least-squares on <i>F</i> ²	full-matrix least-squares on <i>F</i> ²	full-matrix least-squares on <i>F</i> ²
goodness of fit on <i>F</i> ² ^a	1.116	1.026	1.37	0.978
final <i>R</i> indices (<i>I</i> > 2 σ (<i>I</i>)) ^a	<i>R</i> 1 = 0.050, <i>wR</i> 2 = 0.130	<i>R</i> 1 = 0.068, <i>wR</i> 2 = 0.156	<i>R</i> 1 = 0.039, <i>wR</i> 2 = 0.100	<i>R</i> 1 = 0.047, <i>wR</i> 2 = 0.068
<i>R</i> indices (all data)	<i>R</i> 1 = 0.082, <i>wR</i> 2 = 0.176	<i>R</i> 1 = 0.138, <i>wR</i> 2 = 0.193	<i>R</i> 1 = 0.069, <i>wR</i> 2 = 0.135	<i>R</i> 1 = 0.113, <i>wR</i> 2 = 0.099

^a *R*1 = $\sum(|F_o| - |F_c|)/\sum|F_o|$; *wR*2 = $[\sum w(F_o^2 - F_c^2)^2/\sum wF_o^2]^{1/2}$; goodness of fit = $[\sum w(F_o^2 - F_c^2)^2/(N_{obs} - N_{param})]^{1/2}$; *w* = $[o^2(F_o) + (g_1P)^2 + g_2P]^{-1}$; *P* = $[\max(F_o^2; 0) + 2F_c^2]/3$.

mixture of **4b** and **4c** in a 1.2:1 ratio. The mixture remained unchanged when irradiated under similar conditions for an additional time of 20 min. **4c**: ¹⁹F NMR (CDCl₃) δ -117.3 (F_o, *J*_{Pt-F_o} = 360 Hz), -159.9 (t, F_p), -163.2 (m, F_m).

Preparation of [Pt(μ -Cl)(C₆F₅)(PPh₃)₂] (5**). Method i.** The synthesis of **5** was performed as described for **3c** (method ii) by ultraviolet irradiation of **3b** through Pyrex glass, but with increased reaction time (14 h) (71% yield).

Method ii. A mixture of *trans*-[PtCl₂(PPh₃)₂] (0.100 g, 0.126 mmol) and *cis*-[Pt(C₆F₅)₂(thf)₂] (0.057 g, 0.085 mmol) in CH₂Cl₂ (40 mL) was refluxed for 24 h. The resulting yellow solution was concentrated to 2 mL, and then ethanol (10 mL) was added to give **5** as a beige solid which was isolated by filtration and air-dried (68% yield). Anal. Calcd for C₄₈H₃₀F₁₀P₂Pt₂: C, 43.68; H, 2.29. Found: C, 44.03; H, 2.31. EI-MS (FAB⁺): *m/z* 1318 ([M]⁺, 30%). IR (cm⁻¹): ν (C₆F₅)_X-sens 812 (vs), ν (Pt-Cl) 285 (m), 280 (sh), 262 (m). ¹⁹F NMR (CDCl₃): δ -120.1 (d, 4F_o, ³*J*_{Pt-F_o} = 400 Hz), -161.75 (t, 2F_p), -164.4 (m, 4F_m).

X-ray Crystal Structure Determination of 1b. Crystal data and other details of the structure analysis are presented in Table 7. A crystal of **1b** was mounted at the end of a glass fiber and held in place with an epoxy resin adhesive. Unit cell dimensions were determined from 20 centered reflections in the range 21 < 2 θ < 30°. Three check reflections re-measured after 45 min showed no decay over the period of data collection. The structure was solved by direct methods. All non-hydrogen atoms were assigned anisotropic displacement parameters and refined without positional restraints. The dichloromethane solvent molecule Cl(1)-C(57)-Cl(2) was refined isotropically, with a partial occupancy of 0.5. No attempts to locate the hydride ligand were made.

X-ray Crystal Structure Determination of 2a. Crystal data and other details of the structure analysis are presented in Table 7. A crystal of **2a** was mounted at the end of a quartz fiber and held in place with a fluorinated oil. Unit cell dimensions were determined from 25 centered reflections in the range 14.6 < 2 θ < 31.1°. Three check reflections re-measured after every 3 h showed no decay of the crystal over the period of data collection. The structure was solved by Patterson methods. All non-hydrogen atoms were assigned anisotropic displacement parameters and refined without

positional restraints, except for the dichloromethane solvent molecule Cl(3)-C(56)-Cl(4), for which interatomic distances were restrained to 1.72 Å; the carbon atom C(56) was refined isotropically. The hydrogen atoms were constrained to idealized geometries and assigned isotropic displacement parameters equal to 1.2 times the *U*_{iso} value of their respective parent carbon atoms. One of the dichloromethane solvent molecules, Cl(3)-C(56)-Cl(4), was refined with a partial occupancy of 0.25. The dinuclear Pt complex shows a disorder over two positions related by a pseudo binary axis located at (1/4, *y*, 1/4). The disorder arises because the periphery of the molecule has a shape that approximates to 2-fold symmetry, with the local symmetry axis parallel to the crystallographic *b* axis. At the center of the molecule, however, the approximate 2-fold symmetry is broken by a significant inclination of the Pt-Pt vector away from the pseudo-2-fold axis. One of the sets of positions is clearly in the majority (87%), and thus, only the positions of the heavy metal atoms of the minor component could be identified from the electron density maps. The addition of these atoms (Pt(1') and Pt(2')) significantly improves the model (*R*1 = 0.0682 and *wR*2 = 0.1559 with Pt(1') and Pt(2') in the model as compared to *R*1 = 0.0949, *wR*2 = 0.2301 and the largest nonassigned electron density peak of 16.27 e Å⁻³ without these atoms). The midpoints between the two platinum congeners of each set lie very near to (1/4, *y*, 1/4) and define a line parallel to the *b* axis of the unit cell. This line also passes near the positions of the atoms C(13), C(16), and F(16), the midpoint between the two phosphorus atoms P(1) and P(2), and the midpoints of the atom pairs C(14)-C(18), C(15)-C(17), F(14)-F(18) and F(15)-F(17). This line is the false symmetry axis which relates the two disordered molecules. For the atom Pt(2) and the ligands bonded to it, the disorder does not generate separate atomic sites, since this part of the molecule has approximately the symmetry of the pseudo-binary rotation axis, and thus no disorder is seen here. In contrast, the pentafluorophenyl groups bonded to the atom Pt(1), and Pt(1) itself, do not comply with this symmetry element; thus, they show more pronounced disorder. Since the ratio of the disorder is 87/13, as mentioned above only the heavy atom of the minor component (Pt(1')) at this end of the molecule has enough electron density to be clearly identified.

The result is such that in the final density maps there are a good number of peaks with density higher than $1 \text{ e}/\text{\AA}^3$ (15 peaks, maximum $1.38 \text{ e}/\text{\AA}^3$; largest difference hole $-2.29 \text{ e}/\text{\AA}^3$), which cannot be successfully assigned but which likely correspond to the carbon and fluorine atoms of the minor component of the disorder. Despite the disorder, the connectivity of the complex molecule is unambiguously established, and the geometric parameters are coherent. No attempts to locate the hydride ligand were made.

X-ray Crystal Structure Determination of 2c. Crystal data and other details of the structure analysis are presented in Table 7. A crystal of **2c** was mounted at the end of a glass fiber and held in place with an epoxy resin adhesive. Unit cell dimensions were determined from 18 centered reflections in the range $22 < 2\theta < 25^\circ$. Three check reflections re-measured after every 45 min showed no decay over the period of data collection. The structure was solved by direct methods. All non-hydrogen atoms were assigned anisotropic displacement parameters and refined without positional restraints, except for the toluene solvent molecule (C(29)–C(33)), for which the interatomic distance C(29)–C(30) was restrained to 1.50 Å. No attempts to locate the hydride ligand were made.

X-ray Crystal Structure Determination of 3c. Crystal data and other details of the structure analysis are presented in Table 7. A selected crystal of **3c** was fixed with epoxy on top of a glass fiber and transferred to the cold stream of the low-temperature device of the diffractometer. Data were collected by the ω -scan method. Three check reflections measured at regular intervals showed no decay over the period

of data collection. The structure was solved by Patterson methods. All non-hydrogen atoms were refined with anisotropic displacement parameters. The hydrogen atoms were constrained to idealized geometries and assigned isotropic displacement parameters of 1.2 times the U_{iso} values of their respective parent carbon atoms. No attempts to locate the hydride ligand were made.

All calculations were performed on a local area VAX cluster (VAX/VMS V5.5) with the SHELXTL-PLUS³⁹ and SHELXL93⁴⁰ software packages.

Acknowledgment. We thank the Dirección General de Enseñanza Superior for financial support (Spain, Projects PB 95-0003-C0 1-2 and PB 95-0792).

Supporting Information Available: Tables of all atomic positional and equivalent isotropic displacement parameters, anisotropic displacement parameters, all bond distances and bond angles, and hydrogen coordinates and isotropic displacement parameters for the crystal structures of complexes **1b**, **2a**, **2c**, and **3c** (31 pages). Ordering information is given on any current masthead page.

OM970581+

(39) SHELXTL-PLUS Software Package for the Determination of Crystal Structures, Release 4.0; Siemens Analytical X-Ray Instruments, Inc., Madison, WI, 1990.

(40) Sheldrick, G. M. SHELXL-93, a Program for Crystal Structure Refinement; University of Göttingen, Göttingen, Germany, 1993.